VTRC
Virginia Transportation Research Council

We Bring Innovation to Transportation

Development of Design Recommendations for Noncontact Hooked Bar Lap Splices for Large Reinforcing Bars

https://vtrc.virginia.gov/media/vtrc/vtrc-pdf/vtrc-pdf/26-R31.pdf

ZACHARY W. COLEMAN, Ph.D., Associate Engineer
Wiss, Janney, Elstner Associates, Inc.

MASON BROWN, Civil Engineering Officer
United States Air Force

CARIN L. ROBERTS-WOLLMANN, Ph.D., P.E., Professor Emerita
Department of Civil and Environmental Engineering, Virginia Tech

ERIC JACQUES, Ph.D., P.Eng., Associate Professor
Department of Civil and Environmental Engineering, Virginia Tech

BERNARD L. KASSNER, Ph.D., P.E., Research Scientist
Virginia Transportation Research Council

Final Report VTRC 26-R31

VIRGINIA TRANSPORTATION RESEARCH COUNCIL
530 Edgemont Road, Charlottesville, VA 22903-2454
vtrc.virginia.gov

Standard Title Page - Report on Federally Funded Project

1. Report No.: FHWA/VTRC 26-R31	2. Government Accession No.:	3. Recipient's Catalog No.:
4. Title and Subtitle: Development of Design Recommendations for Noncontact Hooked Bar Lap Splices for Large Reinforcing Bars		5. Report Date: February 2026 6. Performing Organization Code:
7. Author(s): Zachary W. Coleman, Ph.D.; Mason Brown; Carin L. Roberts-Wollmann, Ph.D., P.E.; Eric Jacques, Ph.D., P.Eng.; and Bernard L. Kassner, Ph.D., P.E.		8. Performing Organization Report No.: VTRC 26-R31
9. Performing Organization and Address The Charles E. Via, Jr. Department of Civil and Environmental Engineering Virginia Polytechnic Institute and State University Blacksburg, VA		10. Work Unit No. (TRAIS): 11. Contract or Grant No.: 119918
12. Sponsoring Agencies' Name and Address: Virginia Department of Transportation 1221 E. Broad Street Richmond, VA 23219 Federal Highway Administration 400 North 8th Street, Room 750 Richmond, VA 23219-4825		13. Type of Report and Period Covered: Final Contract 14. Sponsoring Agency Code:
15. Supplementary Notes: This is an SPR-B report.		

16. Abstract:

On wide bridges, precast concrete pier caps are often constructed in multiple segments and connected on site because of transportation or construction limitations. When these segments are connected through closure joints, contractors use lap splices of straight reinforcing bars. However, the splice lengths of large (e.g., No. 11) straight bars must be very long to develop the yield strength of the bars. The cost of long splices may offset the benefit of using precast concrete. To reduce splice lengths, bridge designers use hooked bars in noncontact lap splices, presuming that hooked bars allow for shorter splice lengths. The use of noncontact splices avoids conflicts during fit-up in the field. However, neither substantial design guidance nor studies of the behavior of hooked bar lap splices in large concrete elements exists to justify this design philosophy.

To develop design guidance for noncontact hooked bar lap splices, 73 large-scale beam-splice specimens were tested to simulate the closure connection between precast pieces. The bond and anchorage parameters of the noncontact hooked bar lap splices varied, including parameters such as the splice spacing, concrete compressive strength, cover depth, casting position, number of spliced reinforcement layers, hook shape, splice length, number of bundled bars, number of lap splices, amount of transverse reinforcement, and dosage of steel fibers. In addition, nonlinear finite element analyses were conducted to investigate the force transfer mechanism in noncontact hooked lap bar splices and predict splice strength over a wider range of splice configurations than tested in the laboratory.

Results indicated that noncontact hooked bar lap splices without transverse reinforcement (e.g., ties) can fail because the eccentricity between lapped bars causes "hook side bulging," a tension failure concentrated at the hooked ends closest to the sides of a beam. In contrast, splices with transverse reinforcement experienced failure modes such as side-face blowout and concrete crushing. Noncontact hooked bar lap splices had weaker splice strengths than contact splices. Nevertheless, hooked bars are an effective means of reducing required splice lengths. On average, the use of steel fibers and increases in lap length, concrete compressive strength, cover, amount of transverse reinforcement, or the number of lap splices allowed for greater stress to be developed in spliced bars. All else being equal, an increase in either bar size or the number of spliced reinforcement layers decreased the stress that could be developed in the spliced bars. A design equation was developed for the minimum required lap length of hooked bars, which uniformly characterizes the influence of the variables over the ranges explored in this study. To enable immediate implementation of the design equation in practice, design examples and proposed code language were also prepared for incorporation into relevant standards.

On completion of this research, the researchers acknowledged the potential of applying the results beyond the project's original scope. Supplemental information on these additional applications can be found at https://library.vdot.virginia.gov/vtrc/supplements.

17. Key Words: accelerated bridge construction, anchorage, bond and development, noncontact lap splice, precast concrete	18. Distribution Statement: No restrictions. This document is available to the public through NTIS, Springfield, VA 22161.

19. Security Classif. (of this report): Unclassified	20. Security Classif. (of this page): Unclassified	21. No. of Pages: 67	22. Price:

Form DOT F 1700.7 (8-72) Reproduction of completed page authorized

FINAL REPORT

DEVELOPMENT OF DESIGN RECOMMENDATIONS FOR NONCONTACT HOOKED BAR LAP SPLICES FOR LARGE REINFORCING BARS

Zachary W. Coleman, Ph.D.
Associate Engineer
Wiss, Janney, Elstner Associates, Inc.

Mason Brown
Civil Engineering Officer
United States Air Force

Carin L. Roberts-Wollmann, Ph.D., P.E.
Professor Emerita
Charles E. Via, Jr.
Department of Civil and Environmental Engineering
Virginia Tech

Eric Jacques, Ph.D., P.Eng.
Associate Professor
Charles E. Via, Jr. Department of Civil and Environmental Engineering
Virginia Tech

Bernard L. Kassner, Ph.D., P.E.
Research Scientist
Virginia Transportation Research Council

In Cooperation with the U.S. Department of Transportation
Federal Highway Administration

Virginia Transportation Research Council
(A partnership of the Virginia Department of Transportation
And the University of Virginia since 1948)

Charlottesville, Virginia

February 2026
VTRC 26-R31

DISCLAIMER

The contents of this report reflect the views of the author(s), who is responsible for the facts and the accuracy of the data presented herein. The contents do not necessarily reflect the official views or policies of the Virginia Department of Transportation, the Commonwealth Transportation Board, or the Federal Highway Administration. This report does not constitute a standard, specification, or regulation. Any inclusion of manufacturer names, trade names, or trademarks is for identification purposes only and is not to be considered an endorsement.

ABSTRACT

On wide bridges, precast concrete pier caps are often constructed in multiple segments and connected on site because of transportation or construction limitations. When these segments are connected through closure joints, contractors use lap splices of straight reinforcing bars. However, the splice lengths of large (e.g., No. 11) straight bars must be very long to develop the yield strength of the bars. The cost of long splices may offset the benefit of using precast concrete. To reduce splice lengths, bridge designers use hooked bars in noncontact lap splices, presuming that hooked bars allow for shorter splice lengths. The use of noncontact splices avoids conflicts during fit-up in the field. However, neither substantial design guidance nor studies of the behavior of hooked bar lap splices in large concrete elements exists to justify this design philosophy.

To develop design guidance for noncontact hooked bar lap splices, 73 large-scale beam-splice specimens were tested to simulate the closure connection between precast pieces. The bond and anchorage parameters of the noncontact hooked bar lap splices varied, including parameters such as the splice spacing, concrete compressive strength, cover depth, casting position, number of spliced reinforcement layers, hook shape, splice length, number of bundled bars, number of lap splices, amount of transverse reinforcement, and dosage of steel fibers. In addition, nonlinear finite element analyses were conducted to investigate the force transfer mechanism in noncontact hooked lap bar splices and predict splice strength over a wider range of splice configurations than tested in the laboratory.

Results indicated that noncontact hooked bar lap splices without transverse reinforcement (e.g., ties) can fail because the eccentricity between lapped bars causes “hook side bulging,” a tension failure concentrated at the hooked ends closest to the sides of a beam. In contrast, splices with transverse reinforcement experienced failure modes such as side-face blowout and concrete crushing. Noncontact hooked bar lap splices had weaker splice strengths than contact splices. Nevertheless, hooked bars are an effective means of reducing required splice lengths. On average, the use of steel fibers and increases in lap length, concrete compressive strength, cover, amount of transverse reinforcement, or the number of lap splices allowed for greater stress to be developed in spliced bars. All else being equal, an increase in either bar size or the number of spliced reinforcement layers decreased the stress that could be developed in the spliced bars. A design equation was developed for the minimum required lap length of hooked bars, which uniformly characterizes the influence of the variables over the ranges explored in this study. To enable immediate implementation of the design equation in practice, design examples and proposed code language were also prepared for incorporation into relevant standards.

On completion of this research, the researchers acknowledged the potential of applying the results beyond the project’s original scope. Supplemental information on these additional applications can be found at https://library.vdot.virginia.gov/vtrc/supplements.

FINAL REPORT

DEVELOPMENT OF DESIGN RECOMMENDATIONS FOR NONCONTACT HOOKED BAR LAP SPLICES FOR LARGE REINFORCING BARS

Zachary W. Coleman, Ph.D.
Associate Engineer
Wiss, Janney, Elstner Associates, Inc.

Mason Brown
Civil Engineering Officer
United States Air Force

Carin L. Roberts-Wollmann, Ph.D., P.E.
Professor Emerita
Charles E. Via, Jr. Department of Civil and Environmental Engineering
Virginia Tech

Eric Jacques, Ph.D., P.Eng.
Associate Professor
Charles E. Via, Jr. Department of Civil and Environmental Engineering
Virginia Tech

Bernard L. Kassner, Ph.D., P.E.
Research Scientist
Virginia Transportation Research Council

INTRODUCTION

The Virginia Department of Transportation (VDOT) has recently begun using noncontact hooked bar lap splices to connect large precast concrete bent caps, as in the Hampton Roads Bridge Tunnel expansion project. Reinforcing bars in precast bent caps are large (e.g., No. 9 and greater), thereby resulting in excessively long cap-to-cap connections if code-specified details (e.g., lap splices of straight bars) are implemented. VDOT and its consulting engineers have hypothesized that hooked bars can transfer tensile forces over shorter lengths than straight bars, allowing for shorter splice lengths and, consequently, narrower closure joints between bent caps. Despite the expected economic benefits and improved speed of construction when using hooked bar lap splices, little to no work has been conducted examining the behavior of lap splices of large, hooked bars.

Noncontact Hooked Bar Lap Splices

Figure 1a illustrates an example of a noncontact hooked bar lap splice. Precast concrete elements are constructed with hooked bars protruding into the joint, where hooks from adjacent elements are overlapped over a length l_s to develop the yield stress of the splice. Noncontact lap

splices are preferred over contact lap splices to prevent interference between opposing hooks during fit-up. Once the hooks are aligned and any necessary transverse reinforcement, such as ties oriented perpendicular to the splices, is added, the sides of the joint are formed, and concrete is cast to complete the connection.

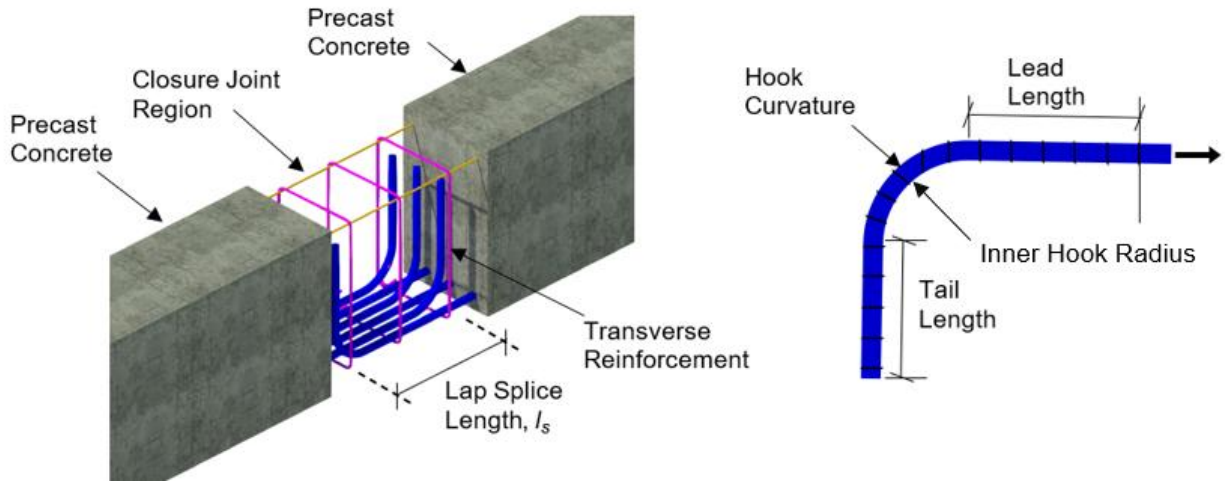

Figure 1. Noncontact Hooked Bar Lap Splices: (a) Isometric View of Two Adjoined Precast Concrete Beams and (b) Hooked Bar Nomenclature

The longitudinal spliced bars can terminate in either a 90° hook, as in Figure 1a, a 180° hook, or a "U-bar" (i.e., continuous hooked reinforcement between the flexural compression and tension zones). As Figure 1b illustrates, the straight portion of a hooked bar is called the "lead length," and the portion extending below the hook curvature is referred to as the "tail length" l_{ext}.

Code-Permitted Connection Details

A Class B lap splice of straight bars is a common method to connect precast concrete elements in compliance with the American Association of State Highway and Transportation Officials (AASHTO) *LRFD Bridge Design Specifications* (AASHTO, 2020). However, Class B lap splices of large reinforcing bars are impractically long to connect precast elements. For example, the absolute minimum required splice length (after all possible beneficial reductions have been accounted for and assuming no excess reinforcement) of an uncoated, bottom-cast, Grade 60, No. 9 bar in normal weight, 4 ksi concrete is about 42 inches. With some allowance for concrete clearance between the ends of the lapped bars and the precast concrete, the required joint length could conceivably be 4 feet. These relatively large closure joints may present construction challenges, increase the required amount of cast-in-place (CIP) concrete, and reduce the speed of using precast concrete.

Background

The Mechanisms of Bond and Anchorage of Reinforcing Bars in Concrete

Hooked bars develop stress through bond and hook end-bearing mechanisms. The bond between deformed bars and concrete is developed through chemical adhesion, friction, and

bearing of the bar deformations against the concrete (American Concrete Institute [ACI] Committee 408, 2012). The following parameters are generally positively correlated with bond strength: concrete compressive strength (Darwin et al., 1995), cover depth (Orangun et al., 1975), amount of transverse reinforcement (Darwin and Graham, 1993), lap and embedment length (Canbay and Frosch, 2005), and steel fiber dosage (Harajli and Salloukh, 1997). Other variables negatively correlate with bond strength, such as the depth of fresh concrete below a bar (Jirsa and Breen, 1981). Various codes treat bundled bars as having reduced bond strength and requiring longer development lengths (AASHTO, 2020; ACI Committee 318, 2019), although this theory has been challenged in various studies (Bashandy, 2009; Cairns, 2013). In addition, although larger bars have greater average bond strengths than small bars, they develop less stress because the cross-sectional area of a reinforcing bar increases more quickly than the surface area over which bond forces act.

In addition to bond forces, hooked bars rely on bearing forces within the hook curvature to achieve their anchorage strength. These bearing forces occur as the hook presses against the concrete along the curved portion of the bar, thereby providing additional anchorage resistance. Consequently, hooked bars can be developed in shorter distances than straight bars.

Researchers have conducted several studies exploring the influence of construction and detailing parameters on the strength of hooked bars anchored in concrete. Marques and Jirsa (1975) investigated whether the hook shape affected anchorage strength and concluded that standard 90° and 180° hooks have equivalent anchorage strengths. For beam-column joints, decreases in the lever-arm distance of the beam containing the hooked bars have been found to increase anchorage strength. Deeper beams generate more inclined struts and greater tension forces along the lead (straight portion) of the hooked bar, reducing anchorage strength (Coleman et al., 2023). Ajaam et al. (2017) also reported that staggered hooks in multiple reinforcement layers have lower average anchorage strengths than identical elements with fewer nonstaggered hooks.

Noncontact Lap Splices of Straight Bars

Several researchers have investigated the behavior of noncontact lap splices of straight bars. They hypothesized that noncontact lap splices transfer forces through in-plane truss mechanisms consisting of inclined compression struts equilibrated by transverse tension ties (McLean and Smith, 1997; Sagan et al., 1991). Sagan et al. (1991) observed that increases in splice spacing up to $6d_b$ did not reduce the splice strength. Other studies that examined more closely spaced spliced bars reported similar results (Chamberlin, 1958; Chinn et al., 1955; Walker, 1951). In contrast, Hamad and Mansour (1996) found that splice spacing influences splice strength, with the greatest strength being achieved when the clear splice spacing was between 20 and 30% of the splice length, approximately $4–6d_b$. Hwang et al. (2022) further observed that splices spaced as little as $2–4d_b$ exhibit different strengths than comparable contact splices. Because of researchers' conflicting claims, the effect of splice spacing on the bond strength of noncontact lap splices of straight reinforcing bars is still uncertain.

Previous Investigations of Hooked Bar Lap Splices

Several studies have examined the strength of contact and noncontact hooked bar lap splices in bridge deck closure joints, but their findings are insufficient to support design recommendations for large, hooked bars. Most studies—such as those by Au et al. (2011), Brush (2004), Dragosavić et al. (1975), French et al. (2011), Jahromi and Azizinamini (2019), Joergensen and Hoang (2015), Ryu et al. (2007), and Sheng et al. (2013)—have focused on the use of hooked bar lap splices in bridge decks, in which small bars are used. Furthermore, standard hooks (AASHTO, 2020) were not used in several of these studies. For these reasons, test data from these studies are insufficient to justify a design procedure for noncontact hooked bar lap splices of large, hooked bars.

Code Guidance for Hooked Bar Lap Splices

Neither ACI Committee 318 (2019) nor AASHTO (2020) *LRFD Bridge Design Specifications* contains language related to hooked bar lap splices. However, the AASHTO (2018) *LRFD Guide Specifications for Accelerated Bridge Construction* permits the use of noncontact hooked bar lap splices in Section 3.6.2.2, provided that (1) the splice length is at least equal to one hooked bar development length (AASHTO, 2020), (2) at least one transverse bar of equal size as the hooked bars is placed in contact with the inner curvature of the hooked bars, and (3) hooks are not spaced farther than 4 inches on center. These provisions are based on tests of small hooks in bridge deck elements (Brush, 2004; French et al., 2011; Sheng et al., 2013), which demonstrated adequate splice performance when the splice length was equal to the hooked bar development length. Because those tests did not predominantly result in splice failures (i.e., the test specimens failed in a mode not related to anchorage, such as flexural crushing of concrete), the level of reliability inherent in the AASHTO (2018) provisions is unknown. Although the AASHTO (2018) provisions are based solely on tests of small bars, they still allow the design of lap splices for large, hooked bars. This design is problematic because no test data exist to justify the safe application of these provisions to large bars.

PURPOSE AND SCOPE

The primary objective of this study was to develop design recommendations guiding the use of noncontact lap splices of large, hooked reinforcing bars in precast concrete elements. To achieve this objective, the force transfer mechanism in noncontact hooked bar lap splices was studied using large-scale experimental tests and nonlinear finite element models. The scope of the work focused on a range of bond parameters aligned with VDOT's intended practice for noncontact hooked bar lap splices. These parameters included using uncoated reinforcing steel with a design yield strength of up to 80 ksi and concrete with a maximum compressive strength of 6 ksi.

METHODS

Overview

The following tasks were executed to achieve the objectives of this research:

- Task 1: Survey practitioners regarding the state of practice of noncontact hooked bar lap splices and identify knowledge gaps.
- Task 2: Experimentally study large-scale beams containing noncontact hooked bar lap splices.
- Task 3: Develop nonlinear finite element models to understand the behavior and variables affecting the strength of noncontact hooked bar lap splices.
- Task 4: Prepare design recommendations and technical commentary for noncontact hooked bar lap splices.

Task 1: State of Practice of Hooked Bar Lap Splices in United States Bridge Infrastructure

A survey pertaining to the state of practice of hooked bar lap splices in bridge infrastructure was disseminated to all 50 state departments of transportation (DOTs). The survey aimed to characterize current practices, examine contemporary design procedures, and identify knowledge gaps related to these splices. It consisted of 10 questions addressing key aspects of their use in bridge design. The survey was sent to each state bridge engineer. However, the recipients were encouraged to consult with colleagues with more relevant expertise, as appropriate.

Following the survey, researchers conducted indepth interviews with representatives from three DOTs recognized for their extensive experience and significant use of noncontact hooked bar lap splices in bridge design. These interviews offered deeper insights into specific challenges and best practices associated with splice design and implementation. See Coleman et al., (2025a) for more information regarding the survey and interviews.

Task 2: Load Tests of Large-Scale Beam-Splice Specimens

Researchers conducted tests to evaluate how key design parameters of hooked bar lap splices, such as splice length and bar size, influence the strength of the connections. The results identified the critical factors affecting splice strength, which were then used to develop descriptive equations for splice strength, leading to design equations and detailing requirements.

To investigate the behavior of noncontact hooked bar lap splices, large-scale beam splice specimens were tested under four-point bending. Figure 2 illustrates the test configuration. Each specimen consisted of two precast concrete segments with protruding hooked bars connected at a central closure joint. The hooked bars extended from the ends of each segment and were embedded within the closure joint to form the splice.

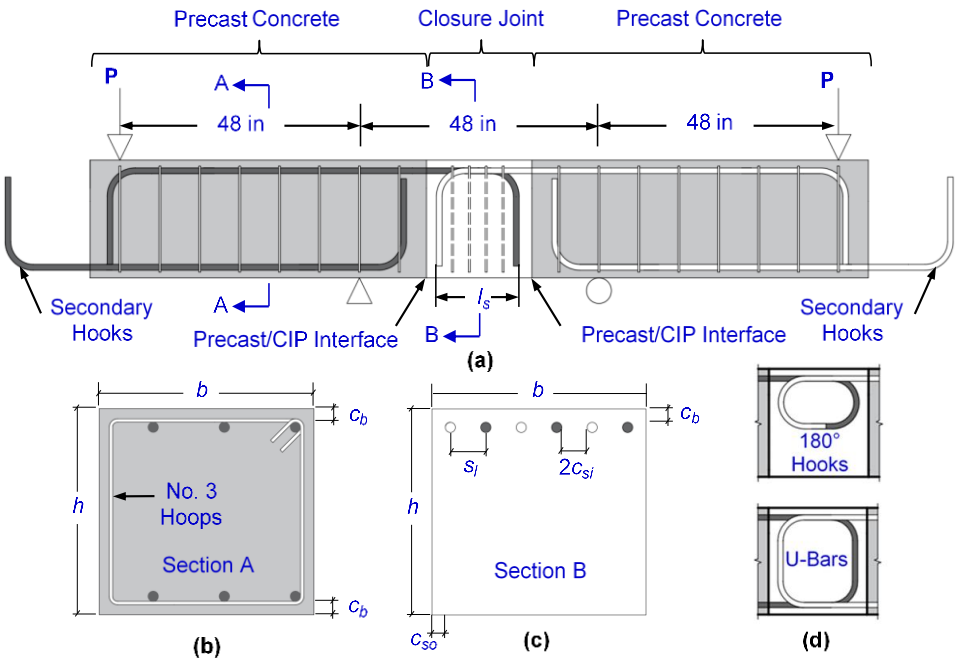

Figure 2. Typical Configuration of Beam-Splice Specimens: (a) Elevation View; (b) Section through Shear Span; (c) Section through Splice Region; (d) Alternative Hook Shape. CIP = cast-in-place.

The interface between the precast and CIP concrete was smooth to create a poor surface condition representing worst-case interface preparation. However, the interface was continuously moistened before CIP concrete placement to mitigate the risk of drying shrinkage. Initial lap lengths l_s were designed to be equal to 80% of the hooked bar development length to ensure that the splice failed before the beam failed in flexure or shear (AASHTO, 2020).

After testing a beam, the closure joint was sawcut to extract the precast segments so that the hooks from the opposite ends of the two segments could be paired to create a second closure joint. Most spliced hooks were bottom-cast. The specimens were inverted for testing so that the tension side faced upward, allowing better access for visual inspection and mapping of crack propagation under load. Each specimen was nominally 13 feet long. For most specimens, the distance from the reaction point to the load point (the shear span) and the distance between the supports (the constant moment region) were each 4 feet. See Brown (2024) and Coleman (2024) for details on the test configuration and specific adjustments.

The test specimens were organized into 13 series to investigate key parameters affecting the hooked bar splice strength f_s. Table 1 summarizes the variables for each series. These parameters included the splice spacing, the presence of transverse reinforcement, the number of layers of spliced hooked bars, the hook shape, the concrete compressive strength, the splice length, the vertical and side cover depth, the flexural beam depth, the casting position, the number of spliced bars, and the use of steel fibers in the closure joint. Each series in Table 1 describes a unique study parameter, which typically differed from the nominal values used for each beam (to be described in the following sections of this report). For example, Series 7 examines the effect of concrete with a compressive strength of 5,000 or 6,000 psi (instead of 4,000 psi—the nominal value) on splice strength.

Table 1. Summary of Experimental Variables

Series No.	Parameter Studied	Description
1	Baseline series	Continuous reinforcement and contact hooked bar lap splices
2	Splice spacing s_l	Inter-splice bar spacing of 4 or 6 inches
3	Transverse reinforcement (parallel ties and lacer bars)	Ties or lacer bars in splice region
4	Transverse reinforcement (perpendicular ties and lacer bars)	Ties with and without lacer bars
5	Number of reinforcement layers	Two layers of noncontact hooked bar lap splices
6	Hook shape	AASHTO standard 90° hooks, 180° hooks, or U-bars (continuous hooked reinforcement between the flexural tension and compression regions)
7	Concrete strength f_{cm}	Cast-in-place compressive strength of 5,000 or 6,000 psi
8	Splice length s_l	Splice lengths of 20 or 25d_b
9	Concrete cover	3 in cover: • Vertical cover only. • Vertical and side cover. • Vertical and side cover with No. 3 ties at 3d_b.
10	Beam depth and casting position	28d_b effective depth • Bottom-cast bars, with or without transverse ties at 3d_b. • Top-cast bars, with or without transverse ties at 3d_b.
11	Bar bundling	Bundled hooks: • All three pairs of hooks. • Only the outermost two pairs of hooks.
12	Number of spliced bars	Lap splices of three or four pairs of noncontact hooked bars
13	Steel fibers in closure	1% fiber dosage by volume with varying cover, transverse reinforcement, and splice spacing

AASHTO = American Association of State Highway and Transportation Officials.

Various configurations of transverse reinforcement were investigated to assess their effect on the behavior of noncontact hooked bar lap splices. These configurations included confining reinforcement oriented perpendicular or parallel to the longitudinal reinforcement, as well as various types of lacer bars. Lacer bars are transverse bars in contact with the inner curvature of the hooked bars and may have straight ends, hooked ends, or be configured as "hairpins" with equal straight lengths. As necessary, lacer bars are rotated and positioned so that the legs and hooks are in contact with the hook curvature of the spliced bars.

Figure 3 illustrates the primary types of transverse reinforcement studied. The perpendicular ties and both types of lacer bars are transverse to the longitudinal spliced reinforcement. Strictly speaking, the parallel ties are not transverse to the longitudinal reinforcement. However, they are transverse to the tails of the spliced hooks. For simplicity, the term "transverse reinforcement" will be used in this report to describe each type of additional reinforcement used.

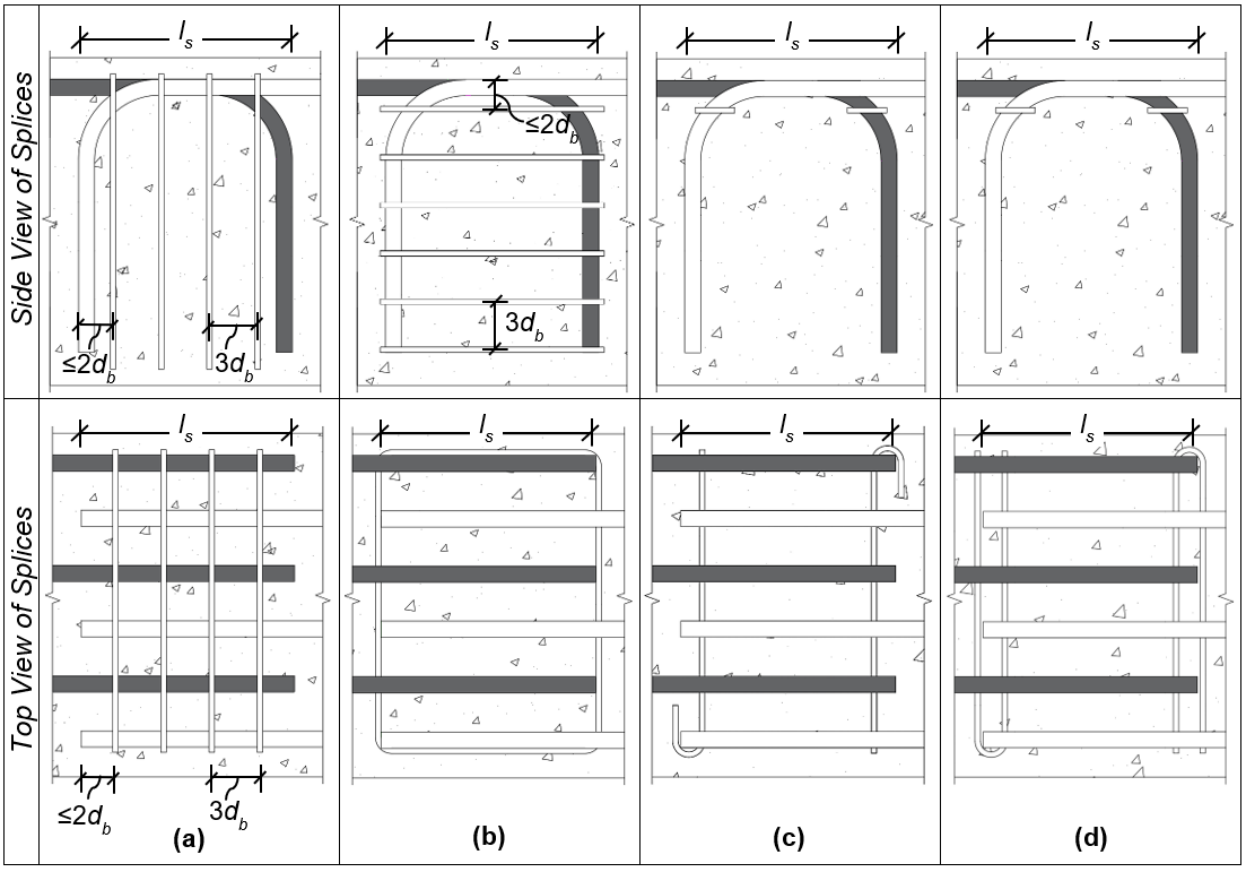

Figure 3. Hooked Bar Lap Splices with Transverse Reinforcement: (a) Perpendicular Ties; (b) Parallel Ties; (c) Hooked Lacer Bars with the Straight Leg Positioned Inside the Bend Radius within the Splice; (d) Hairpin Lacer Bars

The geometric and material parameters for the 73 beams tested in this study are listed in Tables 2 through 4. A three-part naming convention was used to describe the beams in Tables 2 through 4. Consider the name of beam S2-#6-[4 in s_l], the first part (S2) refers to the test series to which the beam belongs, the second part (#6) refers to the imperial nominal bar size of the lapped hooks, and the third part in brackets refers to the characteristic feature of the beam. Thus, S2-#6-[4 in s_l] is a beam from Test Series 2, composed of No. 6 reinforcing bars with a center-to-center splice spacing of 4 inches.

Table 2. Properties of Beam Specimens in Test Series 1 through 4

Series	Beam ID	f_{cm} (ksi)	f_y (ksi)	f_{yt} (ksi)	l_s (in)	b (in)	h (in)	c_{so} (in)	c_b (in)	s_l (in)	n	N	A_{tr1} (in^2)	f_s (ksi)	l_{eq} (in)
1	S1-#6-[Contin.]	3.70	66.1	-	-	24.13	15.75	1.66	1.46	-	3	-	-	76.6	N/A
	S1-#6-[Contact]	4.29	66.1	-	11.33	24.00	15.65	1.57	1.65	0.75	3	-	-	68.2	13.71
	S1-#9-[Contin.]	3.84	71.4	-	-	24.00	23.16	1.69	1.58	-	3	-	-	78.4	N/A
	S1-#9-[Contact]	3.70	71.4	-	17.08	24.00	23.50	1.43	1.80	1.13	3	-	-	49.2	32.81
	S1-#11-[Contin.]	3.80	66.8	-	-	16.63	27.69	1.63	1.58	-	2	-	-	72.0	N/A
	S1-#11-[Contact]	3.69	66.8	-	21.69	17.38	27.88	1.71	1.78	1.41	2	-	-	48.7	47.13
2	S2-#6-[4 in s_l]	3.50	66.1	-	11.29	24.00	15.67	1.74	1.42	4.00	3	-	-	60.1	17.04
	S2-#6-[6 in s_l]	3.50	66.1	-	11.21	34.00	15.78	1.63	1.48	6.06	3	-	-	59.7	17.17
	S2-#9-[4 in s_l]	4.01	70.0	-	16.92	24.06	23.29	1.59	1.46	4.08	3	-	-	47.3	33.42
	S2-#9-[6 in s_l]	4.01	70.0	-	17.00	34.06	23.33	1.72	1.45	5.89	3	-	-	44.3	34.06
	S2-#11-[4 in s_l]	3.65	66.8	-	21.44	16.63	27.69	1.55	1.43	4.11	2	-	-	44.0	53.12
	S2-#11-[6 in s_l]	3.80	66.8	-	21.44	22.63	27.75	1.60	1.63	6.04	2	-	-	42.4	51.05
3	S3-#6-[HL.4 in s_l]	3.75	66.1	72.9	7.92	24.13	15.63	1.79	1.58	4.00	3	2	0.11	58.0	11.94
	S3-#6-[L.4 in s_l]	4.11	66.1	69.5	9.69	24.00	15.46	1.58	1.75	4.10	3	2	0.11	64.7	12.80
	S3-#6-[P.4 in s_l]	4.29	66.1	69.5	9.90	24.19	15.75	1.75	1.63	3.91	3	6	0.11	76.4	10.22
	S3-#6-[P.6 in s_l]	4.29	66.1	69.5	9.83	31.13	15.71	1.75	1.77	6.03	3	6	0.11	81.0	10.36
	S3-#9-[HL.#4.4 in s_l]	3.67	70.0	69.2	12.04	24.19	23.00	1.72	1.59	3.99	3	4	0.20	60.0	20.24
	S3-#9-[L.#4.4 in s_l]	3.84	70.0	69.2	14.89	24.06	23.19	1.67	1.72	4.03	3	2	0.20	59.0	23.25
	S3-#9-[P.4 in s_l]	3.84	70.0	69.5	14.83	24.06	23.15	1.55	1.63	4.01	3	6	0.11	63.2	20.84
	S3-#9-[P.6 in s_l]	3.84	70.0	69.5	15.00	34.31	23.33	1.59	1.77	6.14	3	6	0.11	66.4	21.24
4	S4-#6-[S.4 in s_l]	3.50	66.1	69.5	7.83	24.00	15.70	1.64	1.61	4.04	3	4	0.11	59.5	12.34
	S4-#6-[S.HL.4 in s_l]	3.36	66.1	72.9	8.06	24.00	15.75	1.73	1.51	3.97	3	8	0.11	62.2	10.88
	S4-#9-[S.4 in s_l]	4.01	70.0	69.5	11.92	24.00	23.23	1.45	1.44	4.05	3	4	0.11	60.3	22.66
	S4-#9-[S.HL.#4.4 in s_l]	3.58	61.6	60.6	9.96	24.19	23.31	1.84	1.90	3.88	3	8	0.20	58.9	19.68
	S4-#9-[S.6 in s_l]	3.85	66.3	69.5	11.79	34.5	23.38	1.71	1.49	5.88	3	4	0.11	50.52	24.06
	S4-#11-[S.6 in s_l]	3.69	66.8	69.5	15.06	22.75	27.79	1.64	1.75	5.98	2	4	0.11	42.7	33.96
	S4-#11-[S.8 in s_l]	3.85	66.8	69.5	14.75	28.75	27.75	1.51	1.58	8.11	2	4	0.11	38.9	34.03

- = not applicable; A_{tr1} = area of one leg of transverse reinforcement; b = beam width; c_b = vertical cover; c_{so} = side cover; f_{cm} = concrete compressive strength; f_s = peak stress developed in bars at the critical section based on moment-curvature analysis; f_y = yield strength of hooked bars; f_{yt} = yield strength of transverse reinforcement; h = beam height; l_{eq} = required splice length using Equation 4 to develop yield strength of Grade 60 bars; l_s = splice length; n = number of lapped bars; N = number of legs of transverse reinforcement within one outer hook diameter from splices; s_l = spacing of spliced bars.

Table 3. Properties of Beam Specimens in Test Series 4 through 9

Series	Beam ID	f_{cm} (ksi)	f_y (ksi)	f_{yt} (ksi)	l_s (in)	b (in)	h (in)	c_{so} (in)	c_b (in)	s_l (in)	n	N	A_{tr1} (in^2)	f_s (ksi)	l_{eq} (in)
4	S4-#6-[S.Ends]	3.58	66.1	72.9	7.96	24.19	15.84	1.62	1.64	4.32	3	2	0.11	57.7	13.66
	S4-#6-[S.Ends&Mid.]	3.11	66.1	72.9	7.88	24.25	15.81	1.51	1.45	4.67	3	3	0.11	51.2	14.12
	S4-#9-[S.Ends]	4.53	61.6	72.9	12.13	24.13	23.25	1.62	1.45	4.06	3	2	0.11	51.1	24.52
	S4-#9-[S.#4.4 in s_l]	3.58	61.6	60.6	12.38	24.28	23.25	1.85	1.64	3.96	3	4	0.20	63.9	20.44
	S4-#11-[S.#4.4 in s_l]	3.51	66.4	60.6	17.06	16.69	27.94	1.67	1.74	4.18	2	5	0.20	59.0	27.57
	S4-#11-[S#4.Ends&Mid.]	4.37	66.4	60.6	17.25	16.69	28.06	1.55	1.71	4.45	2	3	0.20	58.2	28.61
5	S5-#6-[2 Layers]	4.29	66.1	-	11.23	24.38	17.13	1.89	1.45	3.94	6	-	-	43.5	N/A
	S5-#9-[2 Layers]	4.06	66.3	-	16.79	24.00	24.63	1.34	1.55	4.07	6	-	-	36.4	N/A
	S5-#11-[2 Layers]	4.06	66.8	-	21.5	16.63	29.13	1.66	1.54	3.83	4	-	-	31.5	N/A
6	S6-#6-[180° Hook]	3.65	66.1	-	11.17	25.00	15.77	2.13	1.62	4.06	3	-	-	61.6	16.01
	S6-#6-[U-bar]	4.29	66.1	-	11.25	24.13	15.73	1.61	1.64	3.97	3	-	-	56.2	14.78
	S6-#11-[180° Hook]	3.80	66.8	-	21.34	16.63	27.69	1.59	1.70	4.09	2	-	-	41.0	50.24
	S6-#11-[U-bar]	3.69	66.8	-	21.44	16.80	28.00	1.56	1.44	4.03	2	-	-	42.6	52.63
7	S7-#6-[5,000 psi f_c']	5.06	66.1	-	10.23	24.13	15.75	1.64	1.48	4.00	3	-	-	64.1	13.99
	S7-#6-[6,000 psi f_c']	5.86	66.1	-	9.25	24.13	15.63	1.72	1.55	3.98	3	-	-	59.2	12.80
	S7-#9-[5,000 psi f_c']	5.06	66.3	-	15.35	24.19	23.25	1.55	1.47	4.14	3	-	-	52.2	29.70
	S7-#9-[6,000 psi f_c']	5.86	66.3	-	13.79	24.13	23.00	1.49	1.56	3.91	3	-	-	52.3	27.36
8	S8-#9-[20d_b l_s]	3.70	137.7	-	21.94	24.13	23.19	1.51	1.42	4.02	3	-	-	60.2	35.06
	S8-#9-[25d_b l_s]	4.29	137.7	-	28.56	24.00	23.25	1.49	1.70	3.85	3	-	-	76.3	31.96
	S8-#11-[20d_b l_s]	3.80	118.5	-	28.38	16.75	27.75	1.68	1.46	3.98	2	-	-	57.3	51.52
	S8-#11-[25d_b l_s]	3.69	118.5	-	35.75	17.13	28.00	1.77	1.63	3.84	2	-	-	56.1	50.40
9	S9-#6-[3 in c_b]	3.65	66.1	-	11.06	24.25	17.13	1.47	3.02	4.11	3	-	-	75.7	16.52
	S9-#6-[3 in c_b & c_{so}]	3.75	66.1	-	8.13	27.13	18.88	3.13	3.02	4.00	3	-	-	59.8	12.81
	S9-#6-[S.3 in c_b & c_{so}]	3.48	66.1	72.9	8.08	27.13	19.00	3.29	3.26	3.94	3	4	0.11	64.8	10.94
	S9-#9-[3 in c_b & c_{so}]	3.65	66.3	-	13.00	27.13	26.07	3.03	3.32	4.14	3	-	-	49.2	27.45

- = not applicable; A_{tr1} = area of one leg of transverse reinforcement; b = beam width; c_b = vertical cover; c_{so} = side cover; d_b = bar diameter; f_{cm} = concrete compressive strength; f_s = peak stress developed in bars at the critical section based on moment-curvature analysis; f_y = yield strength of hooked bars; f_{yt} = yield strength of transverse reinforcement; h = beam height; l_{eq} = required splice length using Equation 4 to develop yield strength of Grade 60 bars; l_s = splice length; n = number of lapped bars; N = number of legs of transverse reinforcement within one outer hook diameter from splices; s_l = spacing of spliced bars.

Table 4. Properties of Beam Specimens in Test Series 9 through 13

Series	Beam ID	f_{cm} (ksi)	f_y (ksi)	f_{yt} (ksi)	l_s (in)	b (in)	h (in)	c_{so} (in)	c_b (in)	s_l (in)	n	N	A_{tr1} (in^2)	f_s (ksi)	l_{eq} (in)
9	S9-#9-[S.3 in c_b & c_{so}]	3.67	66.3	72.9	13.58	27.13	26.25	2.98	3.07	4.25	3	5	0.11	60.5	20.72
	S9-#11-[3 in c_b]	3.85	66.8	-	21.38	16.75	29.38	1.47	3.44	4.14	2	-	-	49.3	51.17
	S9-#11-[3 in c_b & c_{so}]	3.65	66.8	-	21.58	19.63	30.71	3.06	3.03	4.05	2	-	-	53.7	41.30
	S9-#11-[S.3 in c_b & c_{so}]	3.67	66.8	72.9	21.56	19.75	30.75	3.17	3.26	4.04	2	6	0.11	63.0	28.41
10	S10-#6-[28d_b d]	3.65	66.1	-	11.25	24.13	23.25	1.57	1.65	4.03	3	-	-	59.2	16.16
	S10-#6-[S.28d_b d]	3.48	66.1	72.9	8.00	24.00	23.19	1.82	1.55	3.81	3	4	0.11	59.0	12.40
	S10-#6-[TC.28d_b d]	3.67	66.1	-	11.13	24.13	23.25	1.79	1.73	3.90	3	-	-	59.2	15.57
	S10-#6-[TC.S.28d_b d]	3.26	66.1	72.9	8.00	24.00	23.19	1.88	1.51	3.96	3	4	0.11	59.4	12.88
11	S11-#6-[66% Bundled]	3.75	72.9	-	11.21	24.13	15.75	1.57	1.46	3.98	3	-	-	58.8	16.31
	S11-#6-[100% Bundled]	3.91	72.9	-	11.33	24.13	15.75	1.49	1.64	4.17	3	-	-	63.1	15.91
12	S12-#6-[4 Splices]	3.11	66.1	-	10.59	32.00	15.75	1.57	1.56	4.44	4	-	-	55.2	17.62
	S12-#6-[S.4 Splices]	4.37	66.1	72.9	7.84	31.88	15.75	1.84	1.96	3.82	4	4	0.11	66.7	10.79
	S12-#11-[S#4.3 Splices]	5.04	66.4	60.6	17.04	24.25	28.25	1.51	2.00	4.01	3	5	0.20	63.8	23.07
13	S13-#6-[F.4 in s_l]	4.98	66.1	-	6.15	24.13	15.88	1.77	1.68	3.93	3	-	-	69.8	N/A
	S13-#6-[S.F.4 in s_l]	3.29	66.1	72.9	5.92	24.06	16.06	1.63	1.83	4.38	3	3	0.11	64.0	N/A
	S13-#9-[F.4 in s_l]	3.29	61.6	-	9.67	24.25	23.25	1.89	1.56	3.93	3	-	-	59.0	N/A
	S13-#9-[S.F.4 in s_l]	3.20	61.6	72.9	10.04	24.13	23.25	1.50	1.71	4.29	3	4	0.11	60.8	N/A
	S13-#9-[F.3 in c_b & c_{so}]	4.56	61.6	-	8.63	27.13	26.25	3.18	3.24	4.19	3	-	-	69.8	N/A
	S13-#9-[S.F.3 in c_b & c_{so}]	3.80	61.6	72.9	8.92	27.13	27.00	3.51	3.57	3.72	3	4	0.11	59.0	N/A
	S13-#9-[F.6 in s_l]	3.55	66.3	-	11.88	34.25	23.40	1.46	1.62	6.17	3	-	-	56.3	N/A
	S13-#11-[F.8 in s_l]	5.01	66.8	-	15.30	28.63	27.75	1.52	1.60	8.30	2	-	-	64.3	N/A

- = not applicable; A_{tr1} = area of one leg of transverse reinforcement; b = beam width; c_b = vertical cover; c_{so} = side cover; d = effective beam depth; d_b = bar diameter; f_{cm} = concrete compressive strength; f_s = peak stress developed in bars at the critical section based on moment-curvature analysis; f_y = yield strength of hooked bars; f_{yt} = yield strength of transverse reinforcement; h = beam height; l_{eq} = required splice length using Equation 4 to develop yield strength of Grade 60 bars; l_s = splice length; n = number of lapped bars; N = number of legs of transverse reinforcement within one outer hook diameter from splices; s_l = spacing of spliced bars.

Abbreviations were used in the bracketed terms to provide additional information about characteristic properties of a given test specimen:

- "F." indicates that a 1% dosage of steel fibers by volume was used in the CIP concrete.
- "HL." designates that two hairpin lacer bars were used to enclose the edge hooks.
- "L." indicates that two 180° hooked lacer bars were used to enclose the edge hooks.
- "P." designates that ties parallel to the hook leads (i.e., the straight, continuous portion of bar) were used.
- "S." indicates that ties perpendicular to the hook leads were used. No. 3 reinforcing bars were the default transverse reinforcement in this study and are not noted in the bracketed term. However, in some test specimens, No. 4 bars were used, indicated by "#4" in the bracketed term.
- "TC." indicates that the spliced hooks were top-cast.

Some bracketed terms indicated additional characteristic features in the beams:

- "Contin." refers to the use of continuous bars instead of hooked bar lap splices.
- "Contact" refers to the use of contact lap splices instead of noncontact lap splices.
- "S.Ends" indicates that a perpendicular tie was placed at $2d_b$ from either splice end.
- "S.Ends&Mid." indicates that a perpendicular tie was placed at the middle of the splice and at $2d_b$ from either splice end.
- "U-bar" means the specimen contained U-bars in place of 90° hooks.
- "180° Hook" means the specimen contained 180° hooks in place of 90° hooks.
- "66% Bundled" refers to beams in which the two pairs of edge lap splices were bundled.
- "100% Bundled" refers to beams in which all lap splices were bundled.
- "2 Layers" refers to the use of two layers of staggered hooks in the beam with a 1.5-inch clear spacing between them, instead of one layer.

Across the test matrix, three different sizes of hooked bars—No. 6, No. 9, and No. 11—were used to understand the effect of bar size on splice strength. Various nominal properties were established for the test specimens such that changes in those properties across test series could be parametrically studied. Concrete with a specified 28-day strength of 4,000 psi was nominally used with a cover of 1.5 inches. For most beams, the number of lap splices (n) of No. 6 and No. 9 bars was three, whereas the number of lap splices of No. 11 bars was two to mitigate the risk of a shear failure while using the same testing setup.

Most longitudinal reinforcement in the beam-splice specimens was Grade 60 uncoated reinforcing bars. Although VDOT typically uses uncoated, steel corrosion-resistant reinforcement, it was determined that this difference in reinforcement type would not significantly affect the results of this research. The effect of high-strength reinforcement that VDOT may use in practice—as inferred by using longer lap lengths—was investigated in Series 8, which featured Grade 100 bars. This grade was included to evaluate the performance of higher strength reinforcement, which is similar to the materials VDOT often uses.

Most spliced bars were terminated with a standard 90° hook, as specified by AASHTO (2020). Standard 180° hooks and U-bars (continuous reinforcement between the flexural tension

and compression zones with two standard-hook bends—Figure 2d) were used in the four specimens of Series 6 to investigate the effect of hook shape on splice strength. All shear and transverse reinforcement consisted of uncoated Grade 60 reinforcing bars. The yield strength of all reinforcement types was determined in accordance with ASTM A370 *Standard Test Methods and Definitions for Mechanical Testing of Steel Products* (ASTM International, 2022).

All concrete used in this study was air-entrained concrete with a 5 to 8% target air content and #68 coarse aggregate. All specimens had a target concrete compressive strength of 4,000 psi, except for Series 7, which examined the influence of varying compressive strength on splice strength. The concrete compressive strength f_{cm}, splitting tensile strength, and static modulus of elasticity were determined at the time of specimen testing in accordance with ASTM C39 *Standard Test Method for Compressive Strength of Cylindrical Concrete Specimens* (ASTM International, 2020), ASTM C496 *Standard Test Method for Splitting Tensile Strength of Cylindrical Concrete Specimens* (ASTM International, 2017), and ASTM C469 *Standard Test Method for Static Modulus of Elasticity and Poisson's Ratio of Concrete in Compression* (ASTM International, 2014), respectively. BEKAERT 3D 80/30BGP steel fibers (aspect ratio of 80 and 1.18 inches in length) were used for all specimens in Series 13, which examined the influence of fiber reinforced concrete on splice strength. Brown (2024) and Coleman (2024) report more indepth information about the concrete and steel materials used in each beam.

All beams were tested following the same protocol, with load applied in roughly one-tenth increments of the expected failure load. Between each increment, the loading was paused for approximately 5 minutes to permit crack mapping. The maximum crack width of the two concrete interfaces was recorded periodically before imminent failure of each beam. Linear potentiometers were used to monitor deflections at midspan and under both points of load application. Tests were terminated after the load declined by about 15% of its peak value.

The peak splice stress f_s was determined for each specimen using a moment-curvature analysis. A parabolic concrete constitutive law (Hognestad, 1951) was used with the values of concrete strain at peak strength recommended by ACI Committee 408 (2012) and the measured concrete compressive strengths of Tables 2 through 4. The measured constitutive relationships for all reinforcing steel were used in the moment-curvature analyses. The applied moment used in each analysis was calculated at the splice ends (i.e., the critical section) and accounted for the effects of (1) the applied loading, (2) the self-weight of the specimen, and (3) the self-weight of testing equipment at the points of loading application.

Although the test series in Table 1 were designed to isolate the effects of individual splice parameters on splice strength, variations in concrete compressive strength and splice length between specimens made direct comparisons difficult. To address this challenge, the splice strengths f_s from Tables 2 through 4 were normalized by $f_{cm}^{0.33}$ and $l_s^{0.67}$, for which the exponents 0.33 and 0.67 reflect the influence of concrete compressive strength and splice length on splice strength, respectively. These exponents were determined based on a multivariable regression analysis of all test results, which will be discussed in the section on the results for Task 4.

Task 3: Finite Element Analyses and Parametric Studies

Modeling Approach and Validation Exercises

Nonlinear finite element analyses were performed using the program *FE-Multiphys* (Koutromanos and Farhadi, 2018). The objectives of the finite element analyses were to (1) further understand the mechanism of force transfer in noncontact hooked bar lap splices, (2) investigate the effect of anchorage parameters not within the experimental test matrix on splice strength, and (3) examine the effect of transverse reinforcement detailing on splice strength. Refer to Coleman et al. (2025b) for additional information about the finite element analyses conducted in this research.

Figure 4 shows a typical finite element model of a specimen containing noncontact hooked bar lap splices. Models generally included precast concrete, interface concrete, CIP concrete, hooked tension reinforcement, compression reinforcement, and transverse hoops for shear resistance. The nonlinear, triaxial constitutive concrete model formulated by Moharrami and Koutromanos (2016) was used for all three types of concrete. The constitutive law proposed by Kim and Koutromanos (2016) was used for all steel reinforcement. To capture the effects of imperfect bond on the strength and stiffness of beams containing hooked bar lap splices, reinforcing bars were discretely modeled using beam elements and embedded in three-dimensional solid concrete elements using zero-length bond elements. Figure 5a illustrates this approach for a hooked bar. Slip between the reinforcing bars and concrete is accommodated using the bond elements with the constitutive relationship Murcia-Delso and Shing (2015) proposed (Figure 5b). This study did not determine the experimental bond-slip behavior. Therefore, the empirical formulas recommended by Murcia-Delso et al. (2013) were used to determine the key values of bond stress τ and slip s in the constitutive relationship (τmax, speak, and sr). Perfect bond conditions were assumed in the two directions normal to the beam elements. As with the lapped bars, all transverse reinforcement was modeled as beam elements connected to the surrounding concrete elements with bond elements defined by the Murcia-Delso and Shing (2015) constitutive relationship.

Researchers conducted a preliminary validation study on pullout tests to ensure the adopted simulation scheme could capture the failure modes and peak loads associated with the bond-slip mechanism. The first analysis on specimen 1.4 tested by Eligehausen et al. (1982) involved a No. 8 deformed bar embedded in an unconfined concrete prism, which failed because of splitting tension. The second analysis on specimen M1a tested by Lundgren (2000) involved a No. 5 bar in a concrete prism confined by a steel jacket, which failed because of bar pullout (local slip). The accuracy of the models was assessed by comparing the numerical load-slip behavior with the experimental results the authors reported.

This approach was then validated for hooked bars in noncontact lap splices using the experimental results of specimens S2-#9-[4 in s_l], S3-#6-[HL.4 in s_l], S4-#6-[S.HL.4 in s_l], and S6-#6-[180° Hook]. Parametric analyses were subsequently conducted to examine the influence of beam depth, the number of lap splices, and tail length on the strength of noncontact hooked bar lap splices. Researchers then examined the effects of perpendicular tie location and lacer bar

detailing on splice strength. The axial stresses in parallel ties were analyzed to understand the effect of tie location on the effectiveness of improving anchorage strength.

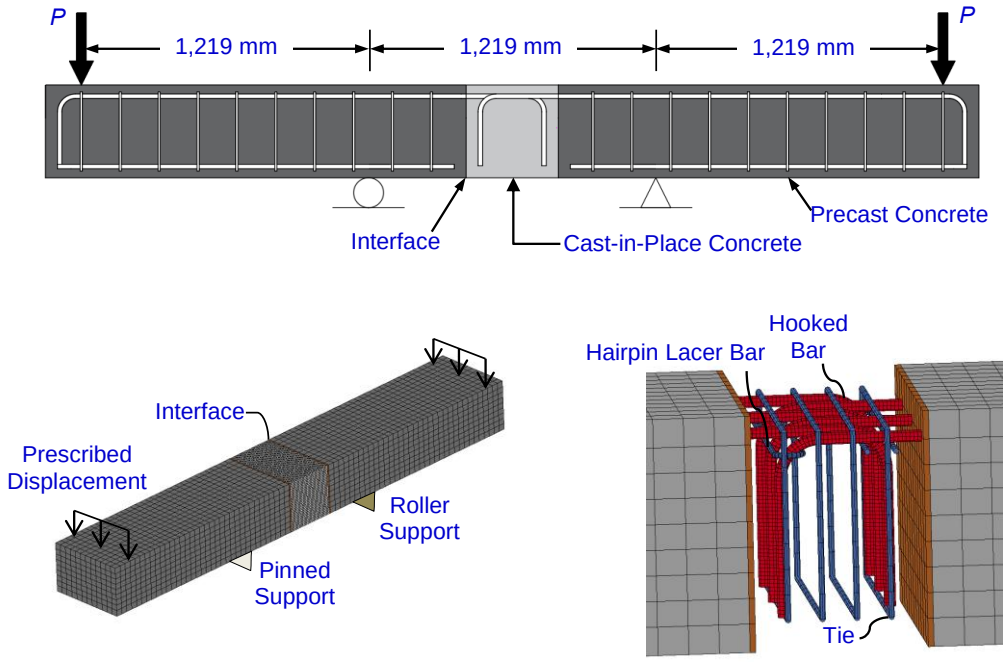

Figure 4. Configuration and Model of Beam-Splice Specimens: (a) Test Specimen; (b) Mesh and Boundary Conditions; (c) Closure Joint. Cast-in-place concrete omitted for clarity.

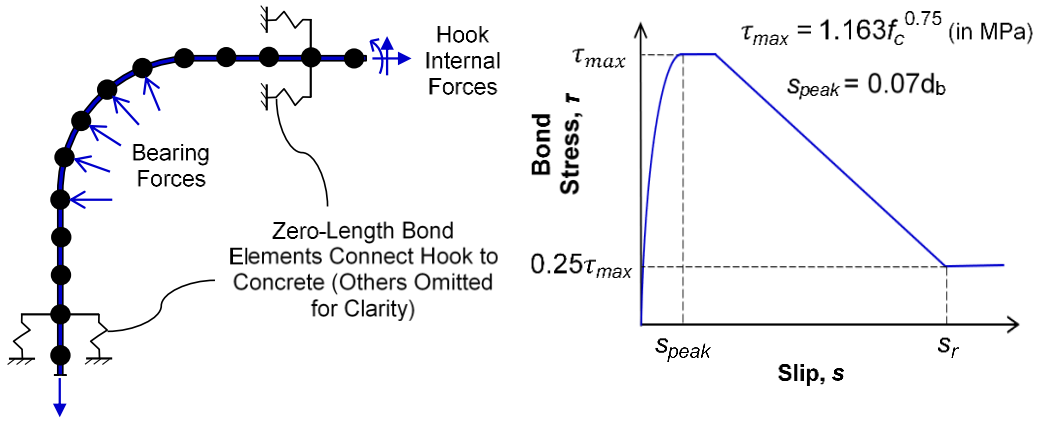

Figure 5. Modeling Imperfect Bond of Hooked Bars: (a) Element Configuration and (b) Bond-Slip Constitutive Law from Murcia-Delso and Shing (2015)

The measured concrete compressive strength f_{cm}, static modulus of elasticity E_c, and splitting tensile strength f_t were used to determine the concrete constitutive relationships for each specimen. A Mode-I fracture energy GF of 0.86 lb/in and a crushing energy of 50 lb/in were used to avoid spurious mesh-size effects. The interface between the precast pieces and the closure joint was modeled in Figures 4b and 4c as a layer of solid elements with material properties identical to those of the precast concrete, apart from the tensile strength, which was set equal to zero. Table 5 lists the material properties of the steel and concrete used in the four

validation specimens: S2-#9-[4 in s_l], S3-#6-[HL.4 in s_l], S4-#6-[S.HL.4 in s_l], and S6-#6-[180° Hook]. Table 6 lists the concrete properties for the two pullout tests. Coleman (2024) reports the material properties for all beams.

Table 5. Properties of Reinforcing Steel in Finite Element Validation Models

Specimen Type	Reinforcement	E_s (ksi) [a]	f_y (ksi)	f_{sh1} (ksi)	f_u (ksi)	ε_{sh}	ε_{sh1}	ε_u
Pullout	No. 5 Bars	29,000	72.5	111.2	116.7	0.0070	0.0500	0.1000
	No. 8 Bars	29,000	60.0	92.1	96.6	0.0085	0.0500	0.1000
Beam	No. 3 Bars	29,000	72.9	111.8	117.3	0.0070	0.0500	0.0910
	No. 6 Bars	29,000	66.1	101.4	106.4	0.0066	0.0500	0.1000
	No. 9 Bars	29,000	69.5	106.6	111.9	0.0052	0.0500	0.0950

E_s = modulus of elasticity; f_{sh1} = stress at one point on hardening regime; f_u = ultimate strength; f_y = yield strength; ε_{sh} = strain at onset of hardening; ε_{sh1} = strain at one point on hardening regime; $\boldsymbol{\varepsilon_u}$ = strain at ultimate strength.

Table 6. Properties of Concrete in Beam-Splice Validation Models

Specimen Type	Specimen ID	Concrete	f_c (ksi)[a]	E_c (ksi)	f_t (ksi)	f_{res} (ksi)	f_0 (ksi)	ε_c	G_F (lb/in)
Pullout	1.4	Cast-in-Place	4.35	3,750	0.26	0.44	2.92	0.0022	0.40
	M1a	Cast-in-Place	5.22	4,100	0.29	0.52	3.50	0.0020	0.63
Beam	S2-#9-[4 in s_l]	Precast	5.21	3,700	0.28	0.52	3.50	0.0023	0.86
		Cast-in-Place	4.00	3,450	0.48	0.41	2.68	0.0021	0.86
	S3-#6-[HL.4 in s_l]	Precast	4.63	3,550	0.25	0.46	3.09	0.0022	0.86
		Cast-in-Place	3.76	3,300	0.38	0.75	2.51	0.0021	0.86
	S4-#6-[S.HL.4 in s_l]	Precast	5.21	3,950	0.25	0.52	3.50	0.0023	0.86
		Cast-in-Place	3.36	3,250	0.36	0.67	2.25	0.0021	0.86
	S6-#6-[180° Hook]	Precast	4.80	3,650	0.30	0.48	3.22	0.0022	0.86
		Cast-in-Place	3.65	3,500	0.41	0.36	2.45	0.0021	0.86

E_c: static modulus of elasticity; f_c: ultimate compressive strength; f_{res} post-peak residual compressive strength; f_t tensile strength; f_0: yield strength of concrete; G_F: Mode-I fracture energy of concrete; ε_c: strain at ultimate compressive strength.

Parametric Studies and Other Simulations

The effects of beam depth, number of lap splices, hook tail length, detailing and placement of lacer bars, location of parallel and perpendicular ties, and joint tensile strength on the strength of noncontact hooked bar lap splices were numerically studied. Compression and shear reinforcement in the precast concrete components were excluded for simplicity.

Parametric Study 1: Effect of Beam Depth

The first study examined how beam height and transverse reinforcement affected splice strength. The objective was to determine if changes in beam depth affected the anchorage strength of hooked bar lap splices, as observed to exist in beam-column joints (Coleman et al., 2023; Johnson and Jirsa, 1981).

Six beams were modeled with three beam heights, those of (1) typical deck panels (8.8 inches), (2) specimen S6-#6-[180° Hook] (15.5 inches), and (3) a beam containing No. 6 bars deeper than those tested in Series 2 of Table 2 (28.4 inches). Models for each height were analyzed for beams with or without transverse reinforcement spaced at $3d_b$ along the splice length. Thus, the only parameters that were varied were the depths of the beams and the presence of transverse reinforcement.

Parametric Study 2: Effect of Number of Lap Splices

The second study examined the effect of the number of lap splices on splice strength because splices with predominantly two or three pairs of lapped hooks were tested in Task 2. This study modeled closure joints with three, five, and seven pairs of lap-spliced bars, maintaining a constant bar diameter of No. 6.

The modeled beams were based on specimen S6-#6-[180° Hook] but with variations in beam width, the number of lap splice pairs, and the presence or absence of transverse reinforcement. The spacing of the lapped bars was held constant at 4 inches. Six beams were modeled, each beam with a different configuration.

The lap splice lengths were adjusted to ensure splice failure. Specimens with transverse reinforcement had a splice length of 11.7 inches, whereas those without transverse reinforcement had a splice length of 7.6 inches. These variations allowed for an assessment of how the number of lap splices and the presence of transverse reinforcement affected overall splice strength.

Parametric Study 3: Effect of Length of Hook Tail

The third study examined whether tail lengths shorter than those in standard hooks reduced splice strength. Shorter tail lengths may reduce the potential for out-of-plumb hooks interfering with each other during fit-up in the field.

The modeled beams were the same as specimen S6-#6-[180° Hook] but with 90° lapped hooks. Researchers analyzed four models for tail lengths of $0d_b$ (just the hook bend), $4d_b$, $8d_b$, and $12d_b$ (i.e., the minimum tail length per AASHTO [2020] *LRFD*).

Parametric Study 4: Effect of Lacer Bar Type

Researchers also conducted a parametric study examining the effects of lacer bar detailing on splice performance. The study's objectives were to identify the type of lacer bar that maximizes splice strength and understand the mechanisms by which lacer bars improve splice strength.

This parametric study examined the effectiveness of four lacer bar configurations: (1) straight lacer bars placed in contact with the inner hook curvature (Figure 6a); (2) hooked lacer bars with the straight leg positioned in contact with the inner hook curvature (Figure 6b); (3) hooked lacer bars with the straight leg contact with the outer hook curvature (Figure 6c); and (4) hairpin lacer bars with equal-length legs enclosing the hooked bars (Figure 6d). A fifth model

was analyzed, which contained no lacer bars to serve as a baseline point of comparison. The lacer bars were modeled using the constitutive properties of No. 3 reinforcing bars shown in Table 5. The geometric and material properties of S3-#6-[HL.4 in s_l] (reported in Tables 1, 4, and 5) were adopted for all simulations in this study.

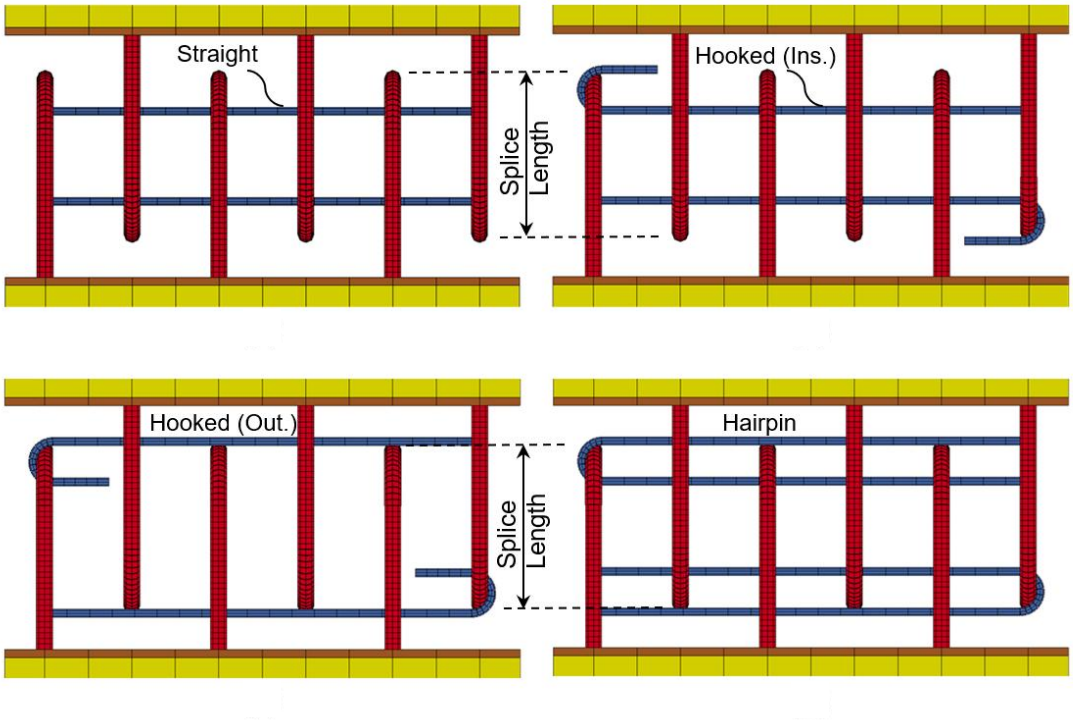

Figure 6. Top View of Lacer Bars Studied Numerically: (a) Straight Lacer Bar; (b) Hooked Lacer Bar (Leg Inside Splice); (c) Hooked Lacer Bar (Leg Outside Splice); (d) Hairpin Lacer Bar

The four lacer bars in Figure 6 were strategically selected to understand the mechanism through which lacer bars improve splice strength. The straight lacer bar was modeled to understand if enclosing the edge spliced bars with the lacer bar was important to improve anchorage strength. The results of this model were compared with the models that contained hooked lacer bars with the leg inside and outside the lap splice. By varying the location of the leg between the two models, the importance of placing the lacer bar in contact with the inner hook curvature as asserted by AASHTO (2018) could be studied. Finally, the model containing hairpin lacer bars was developed to investigate if hairpin lacer bars allowed for greater increases in splice strength than hooked lacer bars.

Parametric Study 5: Effect of Perpendicular Tie Location

Study 5 examined how the location of perpendicular ties (central or closer to splice ends) affects the anchorage strength of noncontact hooked bar lap splices.

In each model, the tie spacing x varied in nine similar increments from ties in direct contact with each other at the center of the splice ($x \approx 0$) to ties positioned at the splice ends adjacent to the hooks ($x = l_s$) (Figure 7). The results for beams with varying perpendicular tie locations were benchmarked against a similar unconfined beam without transverse

reinforcement. Each model had the properties of S3-#6-[S.HL.4 in s_l]. The researchers selected this specimen because the finite element modeling scheme was able to accurately predict the peak load of the specimen, which contained perpendicular ties. The only difference between specimen S3-#6-[S.HL.4 in s_l] and the simulated beams in this parametric study was that all transverse reinforcement was substituted with two perpendicular No. 3 ties positioned along the splice length at a spacing of x.

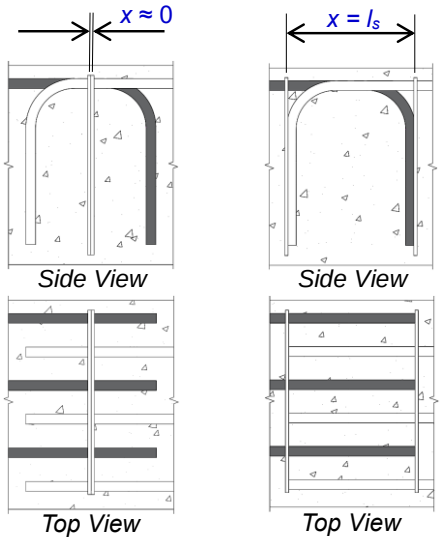

Figure 7. Range of Perpendicular Tie Locations Considered in the Parametric Study

Parametric Study 6: Numerical Simulation Examining the Effect of Parallel Tie Location

One beam was also modeled with parallel ties spaced at $3d_b$, along the height of the hooks in accordance with the requirements of AASHTO (2020), as Figure 3b shows. The observations by Sperry et al. (2017) and Ghimire et al. (2019) motivated this analysis in respective tests of hooked bar and headed bar anchorages in beam-column joints, in which ties within only one outer bend diameter of a standard hook were considered effective to increase anchorage strength. Thus, the objective of this model was to understand the dependence of tie stress (as a proxy for effectiveness to increase splice strength) on tie location relative to the top of the hooked bars. For simplicity and consistency with the parametric study of lacer bars, the geometric and material properties of specimen S3-#6-[HL.4 in s_l] were also used in this model.

Parametric Study 7: Effect of Interface Tensile Strength

During the experimental tests, which served as the foundation for the finite element models, the interface between the precast and CIP concrete was intentionally smooth to simulate poor surface conditions, representing a worst-case scenario for interface preparation. For the computational analyses previously described in this manuscript, the interface tensile strength was set to zero to replicate the as-tested conditions.

However, in practice, precast pieces are often prepared with shear keys or roughened surfaces to facilitate force transfer between the precast and CIP concrete. Because the tests and simulations conducted thus far did not replicate these conditions, it is important to evaluate the

impact of interface treatment on the behavior of noncontact hooked bar lap splices. To explore the potential effect of improved interface conditions on bond performance, specimen S6-#6-[180° Hook] was reanalyzed using an approximately "monolithic interface," in which the interface was assigned the tensile strength equal to the CIP concrete. The results of this model were compared with the original model, termed the "precracked interface," in which no tensile strength was present at the interface.

Task 4: Design Equation for the Splice Lengths of Noncontact Hooked Bars

A descriptive equation characterizing the strength of noncontact hooked bar lap splices was developed using power regression analyses based on data from 58 of the 73 test specimens listed in Tables 2 through 4. Data from Test Series 5 and 13 (multiple reinforcement layers and steel fibers) were excluded and can be addressed in future research. Data from Test Series 1 (continuous reinforcement) were also excluded because the reinforcement was not spliced. Top-cast and bundled bars had the same splice strengths as bottom-cast and nonbundled hooks, which will be discussed in the following sections of this report, so their data were included in the analysis. Data from other studies of hooked bar lap splices could not be used for these analyses for at least one of the following reasons: (1) the lapped bars did not fail in a mode related to anchorage, (2) non-standard hooks were used, (3) the specimens were loaded in direct tension rather than in flexure, and (4) a one-to-one pairing of splices (e.g., two hooks spliced to three opposing hooks) was not provided such that the distribution of tension forces may not be comparable with that examined in this study.

Various forms of a descriptive equation based on analysis of the results of 58 tests were considered to minimize the coefficient of variation (COV) of the test-to-predicted ratios of splice stress. A test-to-predicted stress ratio—defined as the experimental splice strength f_s divided by the predicted strength from the regression equation f_s^p—equal to 1.00 indicates that the calculated stress based on the regression equation is exactly equal to the experimental stress. Thus, an accurate descriptive equation for splice strength can be formulated by constraining the mean test-to-predicted stress ratio to equal 1.00 and minimizing the COV.

RESULTS AND DISCUSSION

Task 1: State of Practice of Hooked Bar Lap Splices in U.S. Bridge Infrastructure

Responses were received from 31 state DOTs, constituting a 62% response rate. The following discussion summarizes key findings from the state of practice survey sent to each state DOT. Figure 8 illustrates the state DOTs' responses when asked what level of experience they have utilizing hooked bar lap splices.

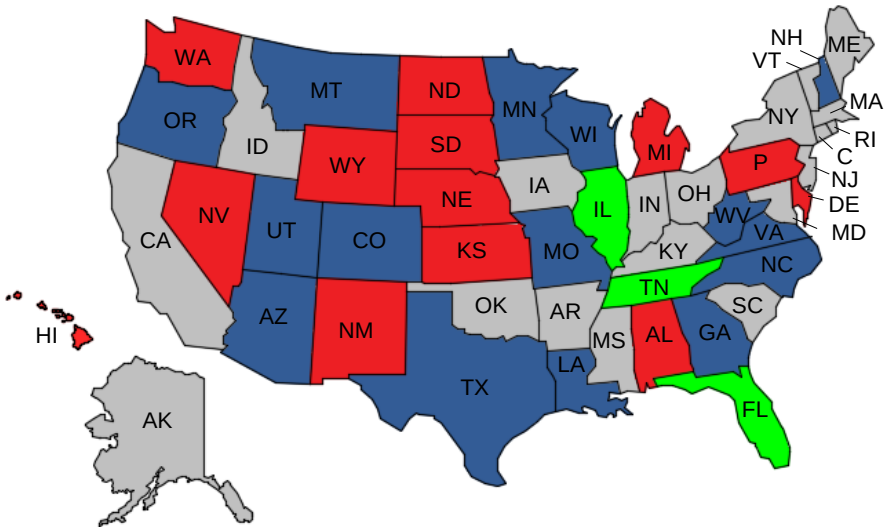

Q1: Does your agency have any experience related to the design of construction of hooked bar lap splices to connect adjacent precast elements?

None (x13) Yes, but very limited (x15) Yes, significant (x3) No response (x19)

Figure 8. Summary of Departments of Transportation Experience Designing with Hooked Bar Lap Splices

Key DOT survey findings include the following:

- More than 50% of respondents have some experience using noncontact hooked bar lap splices, but only three respondents had extensive experience.
- The predominant use of noncontact hooked bar lap splices is in precast deck-to-deck connections. However, they have also been used in continuity diaphragms (Illinois), inverted T-beams, CIP construction (Colorado), and to connect large precast concrete elements (Florida).
- Code provisions for lap splices of straight bars and the development length of hooked bars are typically used to design hooked bar lap splices.
- Hooked bar lap splices are used because they enable narrower closure joints between precast concrete elements, faster construction schedules, and allow for the use of smaller cranes on site.
- Tennessee, Wisconsin, Louisiana, Colorado, Missouri, Montana, West Virginia, North Carolina, and Georgia use provisions from codes intended for lap splices and the development length of hooked bars.
- The lack of a unified, well-known procedure for designing hooked bar lap splices has inhibited more widespread use in bridge infrastructure.

Task 2: Load Tests of Large-Scale Beam-Splice Specimens

Global Load-Deflection Behavior of Specimens

The following summarizes general trends and observed behavior of the tested beam-splice specimens. Brown (2024) and Coleman (2024) report comprehensive test results and beam data for all specimens. The peak bar stress in the closure-joint region achieved before failure f_s is

listed in Tables 2 through 4. Figure 9 includes the typical plots of the applied moment versus midspan deflection of the beam-splice specimens.

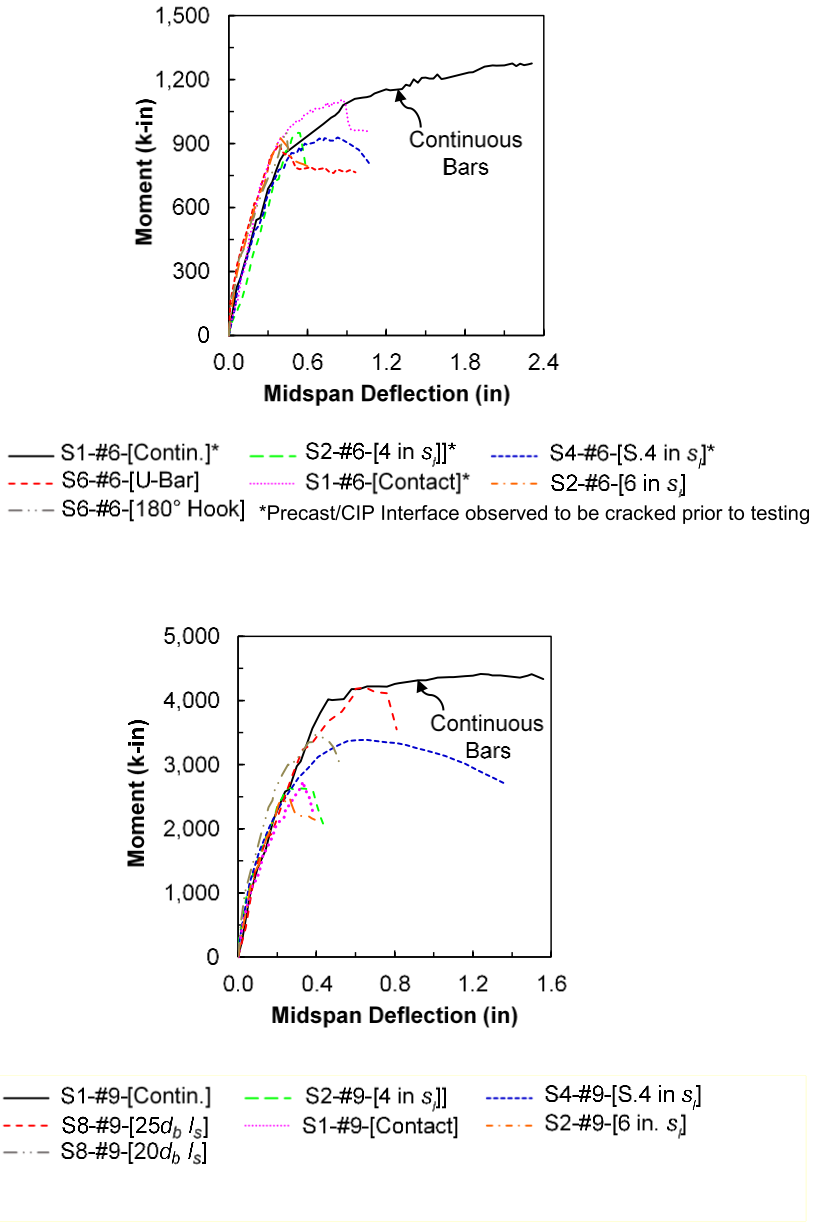

Figure 9. Typical Moment-Deflection Plots of Beams with (a) No. 6 and (b) No. 9 Splices. CIP = cast-in-place.

Specimens with continuous reinforcement (S1-#6-[Contin.] and S1-#9-[Contin.]) exhibited tension-controlled behavior, characterized by yielding and inelastic deformation of the reinforcement. Each specimen with a hooked bar lap splice experienced an anchorage failure. At low loads, specimens with spliced bars exhibited slightly stiffer flexural behavior than those with continuous bars (Figure 9) because spliced specimens have double the reinforcing steel in the closure joint compared with continuous-bar specimens. As the load increased, the stiffness of beams with hooked bar lap splices decreased because of bar slippage, as indicated by wider interface cracks, compared with the stiffness of beams in specimens with continuous bars.

Splices with transverse reinforcement had higher toughness, expressed as the area under the curve, when compared with unconfined splices.

Failure and Resistance Mechanisms of Hooked Bar Lap Splices

Unconfined Lap Splices

Figure 10 shows the typical progression of cracking in the closure joint of beams containing noncontact lap splices.

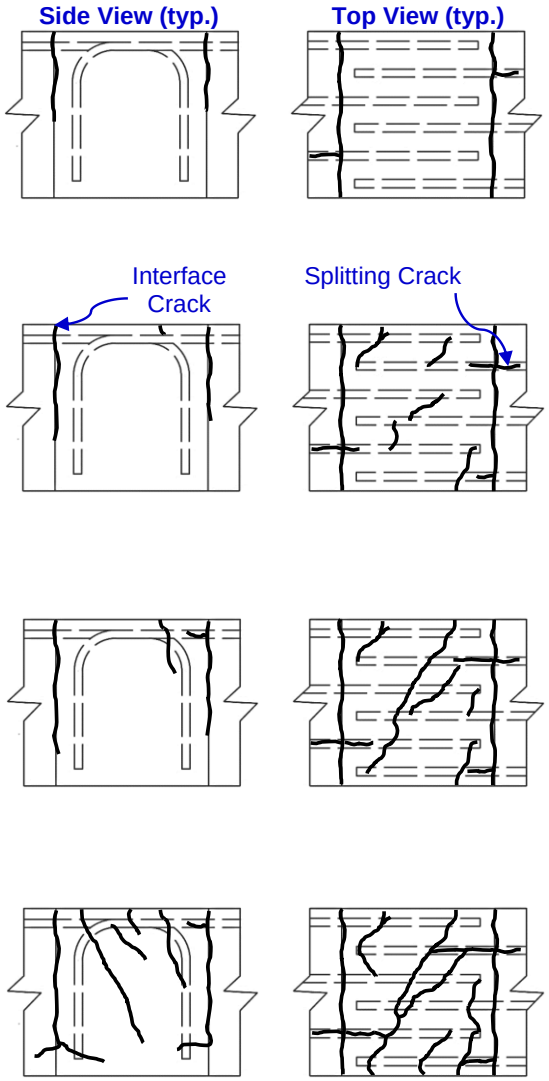

Figure 10. Progression and Extent of Cracking on the Side and Top Faces of Beams with Noncontact Hooked Bar Lap Splices at: (a) ~10% of Ultimate Strength, (b) ~60–70% of Ultimate Strength, (c) ~80–90% of Ultimate Strength, (d) Imminent Failure

At low loads (roughly 10% of the peak moment), transverse cracks originated at the precast and CIP interfaces and propagated to about one-third to one-half of the beam depth. In

addition, at this low level of load, some longitudinal splitting cracks formed slightly outside the closure joint, generally along the interior spliced bars. At higher loads (roughly 60 to 70% of the peak moment), diagonal cracks formed between the spliced bars, and the longitudinal splitting cracks extended into the closure joint.

As the applied load approached 80 to 90% of the peak load, diagonal cracks on the flexural tension face propagated across the entire width of the closure region (Figure 10). Diagonal cracks that had spread to the side face propagated toward the flexural-compression zone, opposite the tail of the exterior hook. These diagonal cracks were most prominent in specimens with transverse reinforcement in the joint. When failure was imminent, the longitudinal splitting cracks on the beam face connected with the diagonal cracks, which had continued to spread across the face and down the beam sides. On the sides of the closure joints, more diagonal cracks appeared, propagating toward the flexural-compression zone, especially for specimens containing transverse reinforcement in the closure joint. In addition, a horizontal crack within the flexural-compression zone typically formed below the tail of the edge hook.

Figure 11 shows photographs illustrating the typical failure mechanisms of noncontact hooked bar lap splices without transverse reinforcement. Failure of these splices was largely attributed to the outward movement of the concrete surrounding the hooked end of an edge bar relative to its lead end (i.e., the continuous end of the bar entering the splice). Simultaneously, for many specimens, the concrete surrounding the hooked end of a spliced bar displaced vertically upward relative to the lead end (Figure 11b). For the three contact lap splices and some noncontact specimens with longer splice lengths from Test Series 8, side-face blowout governed failure (Figure 11c). Common among these specimens was a low relative eccentricity of tension force within a given splice, expressed as the ratio of splice spacing s_l and lap length l_s.

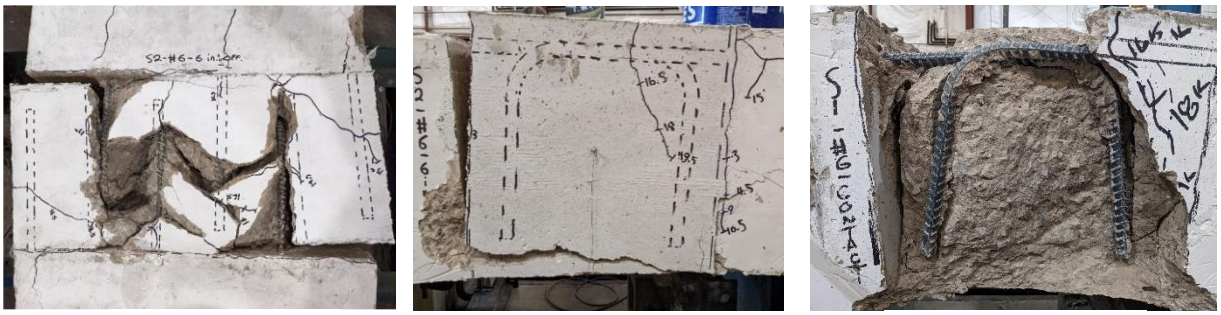

Figure 11. Typical (a) Top and (b) Side Views of Closure Joint at Failure and (c) Side-Face Blowout

Two-dimensional depictions of the hypothesized resistance mechanism in noncontact hooked bar lap are shown in the plane of the splices (Figure 12a) and the plane of the hooks (Figure 12b). The resistance mechanism consists of bearing forces, bond forces, diagonal compression struts, and tension ties. The depictions simplify the three-dimensional flow of forces into two separate two-dimensional representations of the governing behavior. For the sake of simplicity, the representations do not account for interactions between forces developed in the two planes, although such interactions may occur.

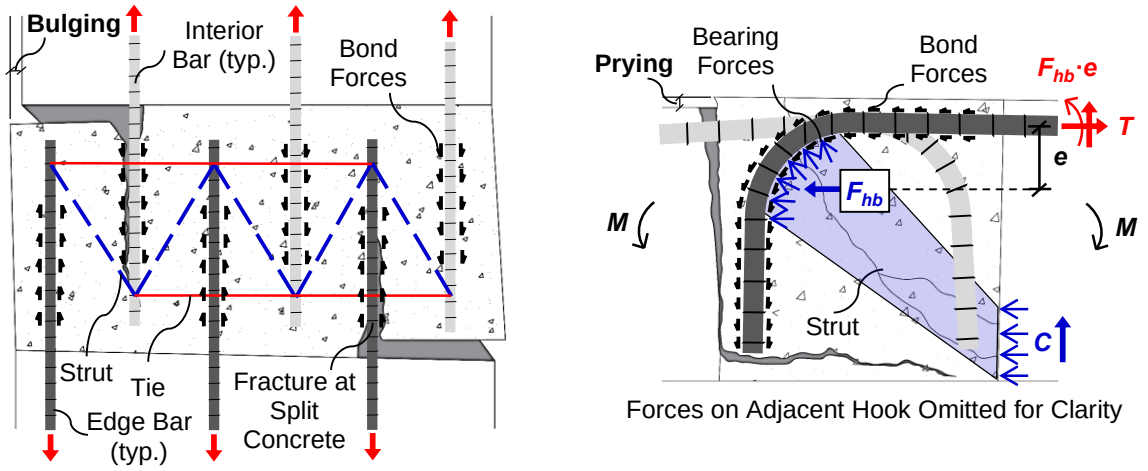

Figure 12. Hypothesized Resistance Mechanisms in Noncontact Hooked Bar Lap Splices in (a) the Plane of the Splices and (b) the Plane of the Hooks

Figure 12a shows the assumed forces acting in the closure joint along the plane of splices. Bond forces along the lead length of the hooks are transferred to adjacent bars through diagonal compression struts and tension ties. As bond forces degrade, compression struts due to hook bearing are assumed to span diagonally from the inner radius of each adjacent hook. For interior bars lapped between two opposing bars, diagonal compression struts on either side provide lateral stabilization. However, for exterior bars, the lateral component of the compression strut acting on an edge bar is unbalanced, necessitating a transverse tension tie to maintain equilibrium.

In an unconfined noncontact hooked bar lap splice, the tensile strength of the concrete cover and a portion of the concrete beneath the spliced bars provide this tension tie. If the capacity of the tie is less than the demand induced by the unbalanced compression strut, the concrete cover will fracture suddenly, causing the hooked ends of the edge bars to displace outward. The term “hook side bulging” is suggested to succinctly designate this failure mode and accompanying resistance mechanism. As Figure 11a shows, the side of the beam near the hooked end of the edge bar appears to bulge outward at failure.

Figure 12b shows the assumed forces acting along the plane of a single hooked bar. The tension force in the bar is developed through a combination of bond stresses along its lead length and the bearing forces within the hook radius. The components of the bearing forces parallel to the bar can be idealized as a single force F_{hb} acting at some eccentricity e defined as the distance from the center of the bar to the idealized bearing force. The product of F_{hb} and e is a moment experienced by the bar, which acts to “pry” the hook upward relative to the lead end of the bar at the precast-CIP interface. Furthermore, the bearing forces developed in the hook radius form a diagonal compression strut spanning from the inner curvature of the hook to the flexural compression zone at the precast-CIP interface. This diagonal compression strut is supported by the diagonal crack pattern observed on the sides of some specimens at failure (Figure 10). The vertical component of this strut acts to push the hooked ends away from the neutral axis, consistent with the displaced shape of the joint after testing (Figure 11b). The term “hook prying” is suggested to succinctly designate this resistance mechanism within the plane of the

hook (Figure 11b). The displaced shape of the side of the beam looks as if the hook has pried upward against the concrete at failure.

This mechanism suggests that a tension field exists in the plane of the hook and parallel to the tail of the 90° hook. This tension field must counteract (1) the positive moment in the bar due to the eccentricity e of the bearing forces F_{hb} and the bar tension T and (2) the vertical component of the strut spanning from the hook to the flexural compression region. The hook tail in the splice anchors the hook against vertical displacement. In some specimens, a horizontal crack under the hook tail, such as the one in Figure 11b, opened prior to failure, consistent with the direction of the hypothesized tension field, as the damaged lap splices show. However, it is unlikely that "hook prying" is the primary failure mechanism. The struts spanning between lapped bars (Figure 12a) are shallower than the struts spanning to the flexural compression zone (Figure 12b), so the predominant resistance mechanism in noncontact hooked bar lap splices likely occurs within the plane of the lapped bars. Thus, "hook side bulging" is the failure mode of noncontact hooked bar lap splices when side-face blowout does not occur. Similar to tail kickout in beam-column joints (Yasso et al., 2021), "hook prying" likely occurs only with other failure modes and does not govern strength.

Lap Splices with Transverse Reinforcement

Figure 13 includes typical views of noncontact lap splices with transverse reinforcement after failure. None of the beams with transverse reinforcement exhibited the "hook side bulging" failure associated with unconfined noncontact hooked bar lap splices. From Figure 12a, such failures are caused by rupturing a tension field perpendicular to the spliced bars. The transverse reinforcement carried that tension, thereby precluding the foregoing failure mode. Therefore, one of the primary roles of transverse reinforcement in noncontact hooked bar lap splices is to carry the transverse tension forces resulting from splice eccentricity.

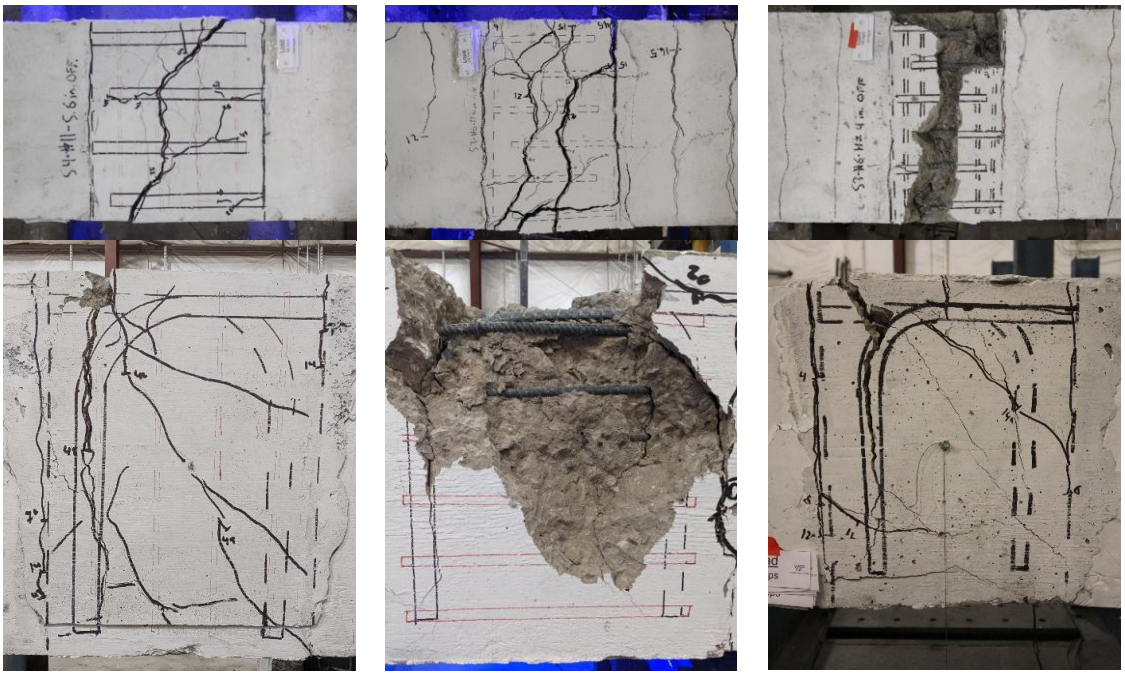

Figure 13. Typical Views of Noncontact Hooked Bar Lap Splices with Transverse Reinforcement after Failure: (a) Perpendicular Ties, (b) Parallel Ties, and (c) Lacer Bars

Influence of Hooked Bar Lap Splice Detailing on Splice Strength

Influence of Splice Length on Splice Strength

Noncontact hooked bar lap splices were generally stronger when splice lengths l_s were longer. The normalized bar stresses at failure, $f_s/f_{cm}^{0.33}$ for noncontact (s_l = 4 in) splices of No. 9 and No. 11 bars are plotted against splice length in Figure 14a. Again, subsequent sections of this report discuss the powers 0.33 and 0.67 in Figure 14. Increasing the splice length generally resulted in stronger lap splices. The strength of the longest splice of No. 11 bars (35.75 inches) was approximately 27% greater than the baseline splice (21.44 inches), and the strength of the longest splice of No. 9 bars (28.56 inches) was 57% greater than the baseline (16.92 inches). It is possible that statistical scatter resulted in the two longer splice lengths of No. 11 bars having roughly the same strength.

Influence of Concrete Compressive Strength on Splice Strength

Hooked bar lap splices with greater concrete compressive strength f_{cm} were stronger than those with weaker concrete compressive strength. The normalized bar stresses at failure $f_s/l_s^{0.67}$ for noncontact (s_l = 4 in) splices of No. 6 and No. 9 bars are plotted against concrete compressive strength f_{cm} in Figure 14b. For the No. 6 bars, splices with a concrete strength of 5.9 ksi were approximately 13% stronger than splices with a concrete strength of 3.5 ksi. For the No. 9 bars, splices with a concrete strength of 5.9 ksi were approximately 28% stronger than splices with a concrete strength of 4.0 ksi.

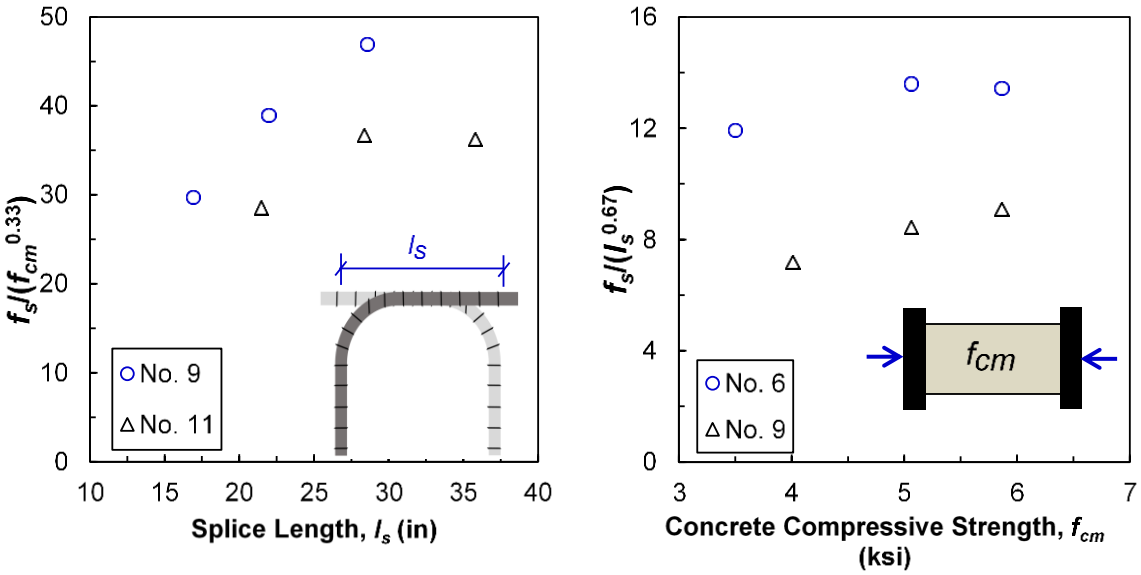

Figure 14. Effect of (a) Splice Length and (b) Concrete Compressive Strength on Normalized Splice Strength for Different Bar Diameters

Influence of Bar Diameter and Splice Spacing on Splice Strength

Noncontact hooked bar lap splices with larger splice spacings s_l and larger bar diameters d_b were weaker compared with those with smaller spacing and smaller diameters. The normalized bar stresses at failure $f_s/(f_{cm}^{0.33}l_s^{0.67})$ for unconfined contact and noncontact splices of No. 6, No. 9, and No. 11 bars are plotted against splice spacing s_l in Figure 15. Two vertical scales are used so that trends in the data can be observed. The left-most axis corresponds to the normalized strengths of the No. 6 bars, and the right-most axis corresponds to the normalized strengths of the No. 9 and No. 11 bars.

For each bar size, noncontact hooked bar lap splices spaced nominally at 6 inches on center were 10% weaker on average than contact lap splices. From Figure 15, an increase in bar size reduced splice strength (expressed as stress). On average, the strengths of the No. 9 and No. 11 splices were only 56 and 47% of the No. 6 splices, respectively. Given the noticeable decrease in splice strength resulting from an increase in bar size, using a greater number of smaller hooked bars is recommended for shorter splice lengths in practice.

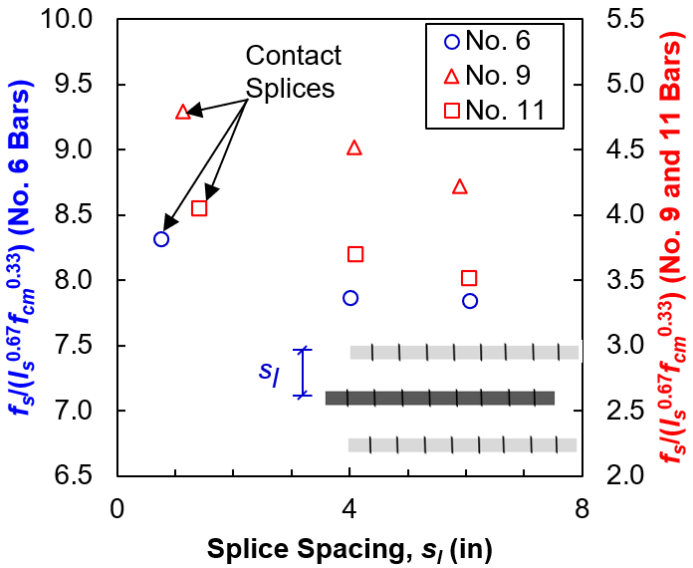

Figure 15. Effect of Bar Size and Splice Spacing on the Reduction of Splice Strength

Influence of Type of Transverse Reinforcement on Splice Strength

Figure 16 shows the normalized bar stresses at failure $f_s/(f_{cm}^{0.33}l_s^{0.67})$ for noncontact splices of No. 6 and No. 9 bars spaced at 4 inches as a function of the type of transverse reinforcement. Compared with the reference beams with unconfined lap splices ("None" in the figure), splices with transverse reinforcement were 13 to 31% stronger for the No. 6 bars and 38 to 64% stronger for the No. 9 bars. Because the same nominal cover (1.5 inches) was used for all beams in this analysis, the ratio of cover-to-bar diameter c/d_b was lower for the beams containing No. 9 bars. Thus, as with lap splices of straight bars (ACI Committee 408, 2012), a larger increase in strength is expected for lower c/d_b ratios, consistent with the aforementioned test results.

Figure 16 also reveals that the hairpin lacer bar (HL.) was more effective at improving splice strength than lacer bars with only a 180° hook (L.). For the specimens containing No. 6 and No. 9 hooks, hooked lacer bars (L.) resulted in a 13 and 38% increase in splice strength, respectively. When hairpin lacer bars were used, the splice strength increased by 20 and 64%, respectively. Thus, hairpin lacer bars are more effective at improving splice strength than hooked lacer bars. This effectiveness is because the second leg of the lacer bar increases resistance to splitting forces and the transverse tension because of splice eccentricity (Figure 12a).

Splices with parallel (P.) and perpendicular (S.) ties resulted in similar increases in splice strength relative to unconfined closure joints ("None" in Figure 16). According to Figure 16, for splices with No. 6 and No. 9 bars, parallel reinforcement resulted in respective increases of 30 and 48% in splice strength, and perpendicular reinforcement achieved respective increases of 26 and 61%. However, it may be preferable to use perpendicular reinforcement in flexural applications to increase shear resistance.

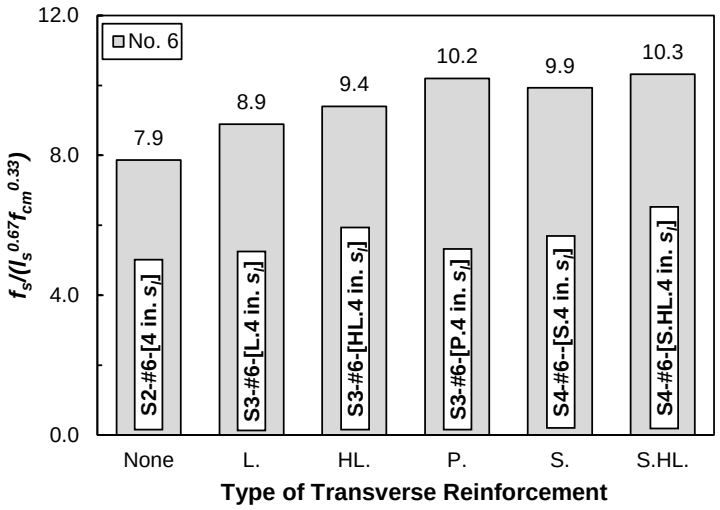

HL. = Hairpin lacer bars; L. = Hooked lacer bars; P. = Parallel ties;
S. = Perpendicular ties; S.HL. = Perpendicular ties with hairpin lacer bars

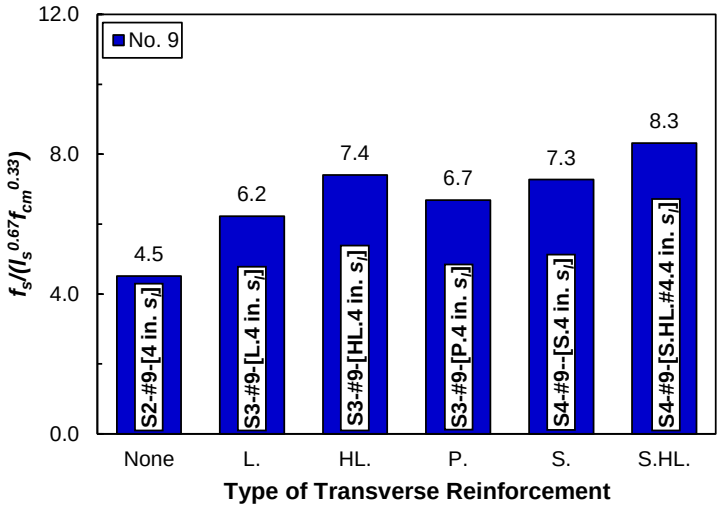

HL. = Hairpin lacer bars; L. = Hooked lacer bars; P. = Parallel ties;
S. = Perpendicular ties; S.HL. = Perpendicular ties with hairpin lacer bars

Figure 16. Effect of Transverse Reinforcement Types on the Increase in Splice Strength for: (a) No. 6 Spliced Bars and (b) No. 9 Spliced Bars

Influence of Hook Shape on Splice Strength

No apparent correlation between splice strength and hook shape was present. The normalized bar stresses at failure $f_s/(f_{cm}^{0.33}l_s^{0.67})$ for noncontact (s_l = 4 in) splices of No. 6 and No. 11 bars are plotted against hook shape in Figure 17. No consistent difference in strength was observed between the 90° and 180° hooks. Because no consistent and substantial difference in strength occurred, no difference in splice strength between the two hook shapes is believed to exist. Although the specimen containing No. 6 U-bars exhibited lower strength than the specimens with 90° or 180° hooks, that trend was not observed for the No. 11 bars. Because only

two specimens containing spliced U-bars were tested, the test results do not confidently indicate a difference in splice strength between U-bars and standard hooks.

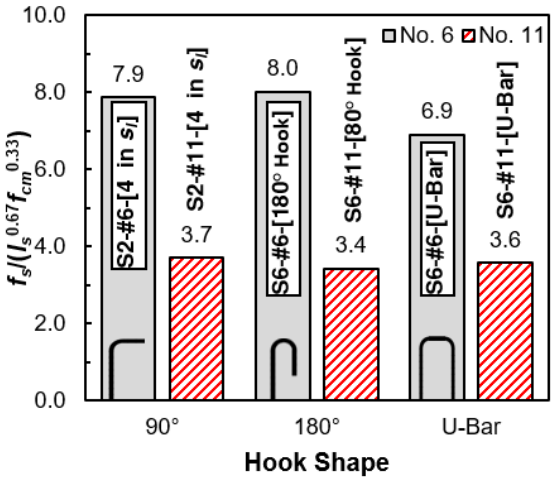

Figure 17. Comparison of Normalized Splice Strengths for Different Hook Shapes and Bar Sizes

Influence of Number of Reinforcement Layers on Splice Strength

An increase in the number of spliced reinforcement layers substantially decreased splice strength. The normalized bar stresses at failure $f_s/(f_{cm}^{0.33}l_s^{0.67})$ for unconfined noncontact (s_l = 4 inches) splices of No. 6, No. 9, and No. 11 bars are plotted against the number of reinforcement layers in Figure 18. On average, the strength of the specimens decreased by roughly 30% when the number of layers of spliced hooks increased from one to two. Regardless of bar size, increasing the number of spliced reinforcement layers decreased the splice strength. This observation differs from those by Jirsa et al. (1995) and Zuo and Darwin (1998), who found that the bond strength of beams containing one layer of contact straight bar lap splices was the same as the bond strength of beams containing two layers.

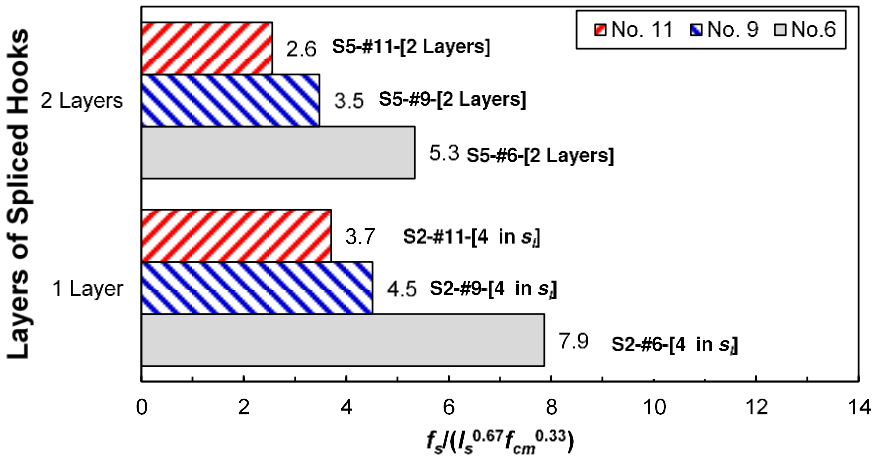

Figure 18. Effect of Splice Layers on the Normalized Strength of Noncontact Hooked Bar Lap Splices for Varying Bar Sizes

Influence of Beam Depth and Casting Position on Splice Strength

Neither an increase in beam depth nor the depth of fresh concrete below the spliced bars affected splice strength. The normalized bar stresses at failure $f_s/(f_{cm}^{0.33}l_s^{0.67})$ for noncontact (s_l = 4 inches) splices of No. 6 bars are plotted against beam depth and the depth of fresh concrete below the spliced bars in Figures 19a and 19b, respectively. Researchers considered both unconfined and confined splices in this analysis. From Figure 19a, regardless of whether transverse reinforcement was used, increasing the effective beam depth from $18d_b$ to $28d_b$ had no substantial effect on splice strength. This result indicates that no noticeable effect of beam depth on anchorage strength exists for hooked bar lap splices. If "hook prying" were to be a failure mechanism in hooked bar lap splices, the expectation was that deeper beams would exhibit lower anchorage strengths. Because the anchorage strengths were not lower, researchers concluded that "hook side bulging" is the governing failure mechanism for splices without transverse reinforcement when side-face blowout does not occur.

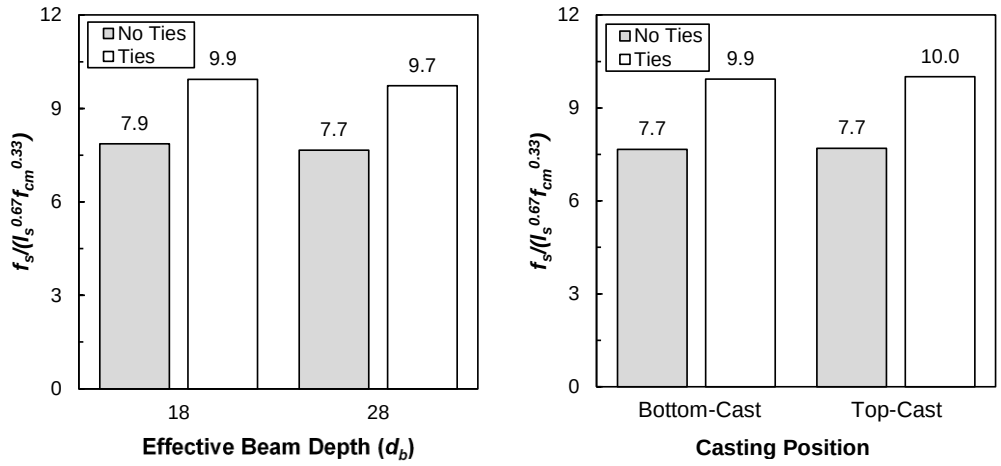

Figure 19. Effect of (a) Beam Depth and (b) Casting Position on Normalized Splice Strength for Noncontact Hooked Bar Lap Splices with and without Transverse Reinforcement

Based on the results plotted in Figure 19b, no top-cast effect similarly exists for hooked bar lap splices. Regardless of whether transverse reinforcement was used, the maximum difference in strength between top-cast and bottom-cast splices was only 2%. Thus, no top-cast effect exists for hooked bar lap splices because stress develops largely because of hook bearing forces near ultimate splice capacity (Coleman, 2024). Therefore, the influence of weaker bond forces along the lead of the bar associated with the top-cast effect should be minimal. In other words, because the failure of hooked bar lap splices is driven either by a tension failure transverse to the splice bars or concrete crushing—neither of which is sensitive to casting position—no top-cast effect should exist for hooked bar lap splices.

Influence of Bar Bundling on Splice Strength

Three beams were tested, each beam with three pairs of spliced bars. One specimen featured noncontact No. 6 hooked bars, the second specimen had the two outermost pairs of bars

bundled, and the third specimen had all three pairs bundled. In all cases, the nominal cross-sectional area of each hooked bar remained constant at 0.44 inch², achieved by using No. 6 bars for the single-bar splices and four-bar bundles of No. 3 bars for the bundled splices.

Consistent with prior research (Bashandy, 2009; Cairns, 2013), lap splices with bundled reinforcing bars demonstrated strength comparable with those having single bars. Figure 20 plots the normalized bar stresses at failure $f_s/(f_{cm}^{0.33}l_s^{0.67})$ for noncontact splices (s_l = 4 inches) against the percentage of bundled bars. All tested splice strengths were within 5% of each other, indicating consistent performance regardless of the degree of bundling.

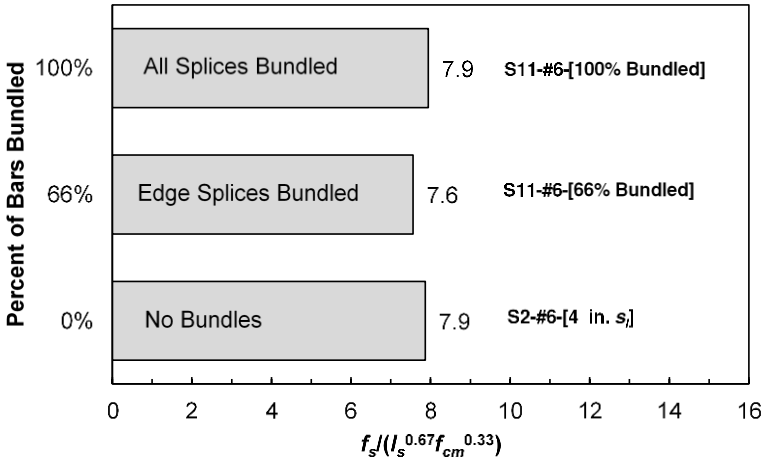

Figure 20. Uniformity in Normalized Splice Strength Regardless of Percentage of Bundled Bars. All specimens had three splices.

This finding suggests that the strength of bundled hooked bar lap splices depends on the combined cross-sectional area of the reinforcement rather than the number of bars in the bundle. The International Federation for Structural Concrete, or *fib*, (2013) recommends this approach for analyzing anchorages of straight bars, focusing solely on the cross-sectional area. However, this design guidance has not yet been incorporated into ACI Committee 318 (2019) or AASHTO (2020) *LRFD*. In other words, the required increase in splice length for three- and four-bar bundles by AASHTO (2020) *LRFD* is not valid for hooked bar lap splices, based on the test results in Figure 20.

Influence of Steel Fibers on Splice Strength

The normalized bar stresses at failure $f_s/(f_{cm}^{0.33}l_s^{0.67})$ for noncontact splices of No. 6, No. 9, and No. 11 bars are plotted against bar size in Figure 21a. Within each bar-size group, the same nominal splice spacing s_l was used. To compare the effectiveness of steel fibers with transverse reinforcement to improve splice strength, test results from other beams in the experimental test matrix were included in the parametric analysis.

From Figure 21a, the use of a 1% dosage of steel fibers increased the splice strength relative to both splices with and without transverse reinforcement, regardless of bar size or splice spacing. Relative to the beams containing splices without transverse reinforcement, the beams

containing steel fibers were 55 to 68% stronger. Compared with the beams containing splices with transverse reinforcement, the beams containing steel fibers without transverse reinforcement were 14 to 52% stronger. Thus, using a 1% dosage of steel fibers in beams containing noncontact hooked bar lap splices can substantially increase splice strength.

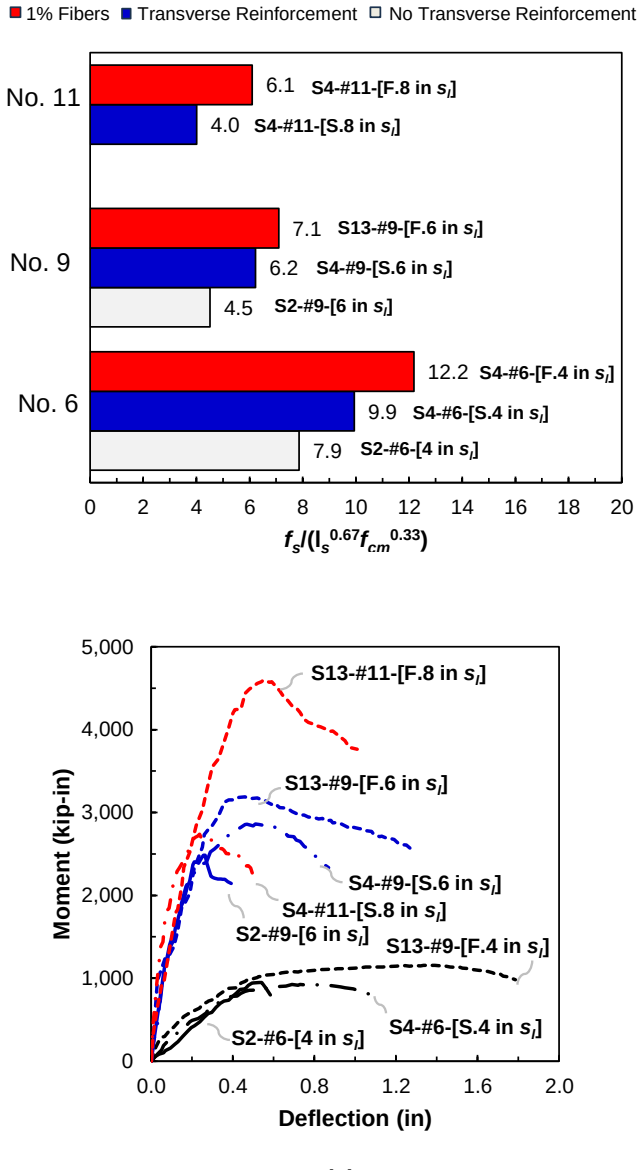

Figure 21. Increase in Strength and Toughness of Hooked Bar Lap Splices due to 1% Fiber Dosage and Perpendicular Ties: (a) Normalized Splice Strengths and (b) Beam Load-Deflection Plots

Note that from Table 4 (S13-#6-[S.F.4 in s_l], S13-#9-[S.F.4 in s_l], and S13-#9-[S.F.3 in c_b & c_{so}]), using transverse reinforcement with the steel fibers did not result in an appreciable increase in strength relative to using only steel fibers. As an example, the normalized splice strength $f_s/(f_{cm}^{0.33} l_s^{0.67})$ for specimen S13-#6-[S.F.4 in s_l], which contained transverse reinforcement, was 13.1 compared with specimen S13-#6-[F.4 in s_l], which did not contain transverse reinforcement, having a normalized strength of 12.2. Therefore, the addition of

transverse reinforcement to hooked bar lap splices embedded in fiber reinforced concrete improved the splice strength by only 7%.

Based on the moment-deflection response of the beams in Figure 21b, using a 1% dosage of steel fibers also substantially increases toughness, expressed as the area under the curve. Considering the beams containing No. 9 bars, for example, the toughness of the beam containing steel fibers (S13-#9-[F.6 in s_l]) was 3,375 kip-in^2, which was approximately five times greater than the toughness of the beam containing unconfined splices (S13-#9-[6 in s_l]). Although this difference is partly because of the difference in load-carrying capacity of the two beams, the greater toughness of beams containing steel fibers is largely driven by the greater post-peak deformability of such splices due to fibers bridging cracks and increased fracture energy. Therefore, using steel fibers may be particularly advantageous when increased capacity for energy dissipation is required.

Task 3: Finite Element Analyses and Parametric Studies

Bond-Slip Validation on Pullout Specimens

Figure 22 presents the results of a preliminary numerical validation study, which involved pullout tests to ensure the simulation could accurately capture the failure modes and peak loads associated with the bond-slip mechanism.

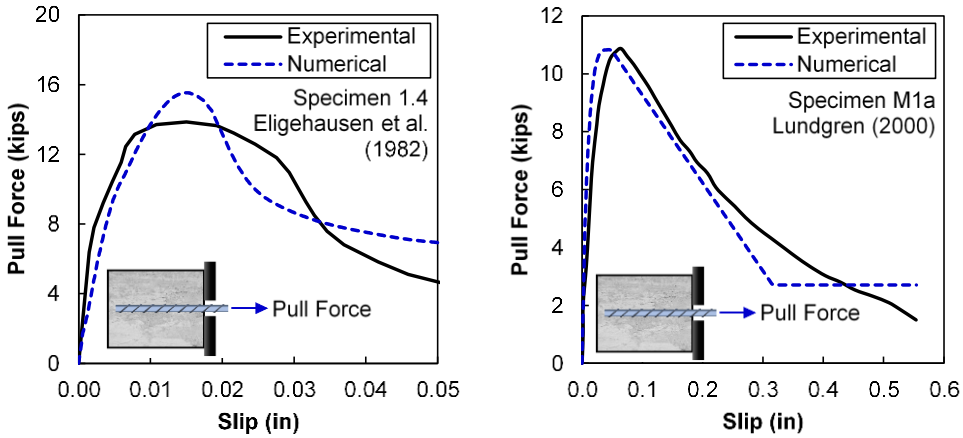

Figure 22. Analysis Results for Validation Pullout Specimens: (a) Eligehausen et al. (1982) Specimen 1.4 and (b) Lundgren (2000) Specimen M1a

The modeled peak capacity of the Eligehausen et al. (1982) specimen was 15.5 kips, approximately 11% greater than the experimental value of 13.9 kips. The modeled peak capacity of the Lundgren (2000) sample was 10.8 kips, comparable with the experimental value of 10.9 kips.

Furthermore, the models correctly captured the failure modes of the two specimens. Specifically, the model of the Eligheausen et al. (1982) sample predicted a splitting failure, and the model of Lundgren's (2000) specimen predicted that strength degradation along the bar-to-concrete interface would lead to pullout. The shape of the load-displacement curve obtained from

the model matches the envelope curve of the bond-slip law in Figure 5b, also supporting the conclusion that strength degradation along the bar-to-concrete interface (i.e., localized concrete crushing) leads to pullout.

Validation on Beam-Splice Specimens

The finite element modeling scheme was then applied to four beam-splice specimens to determine if the models accurately captured the behavior of hooked bar lap splices. Figure 23 compares the numerical and experimental midspan moment versus deflection response of the four beams. The finite element models accurately captured the global moment-deflection behavior and peak load at splice failure of the validation specimens.

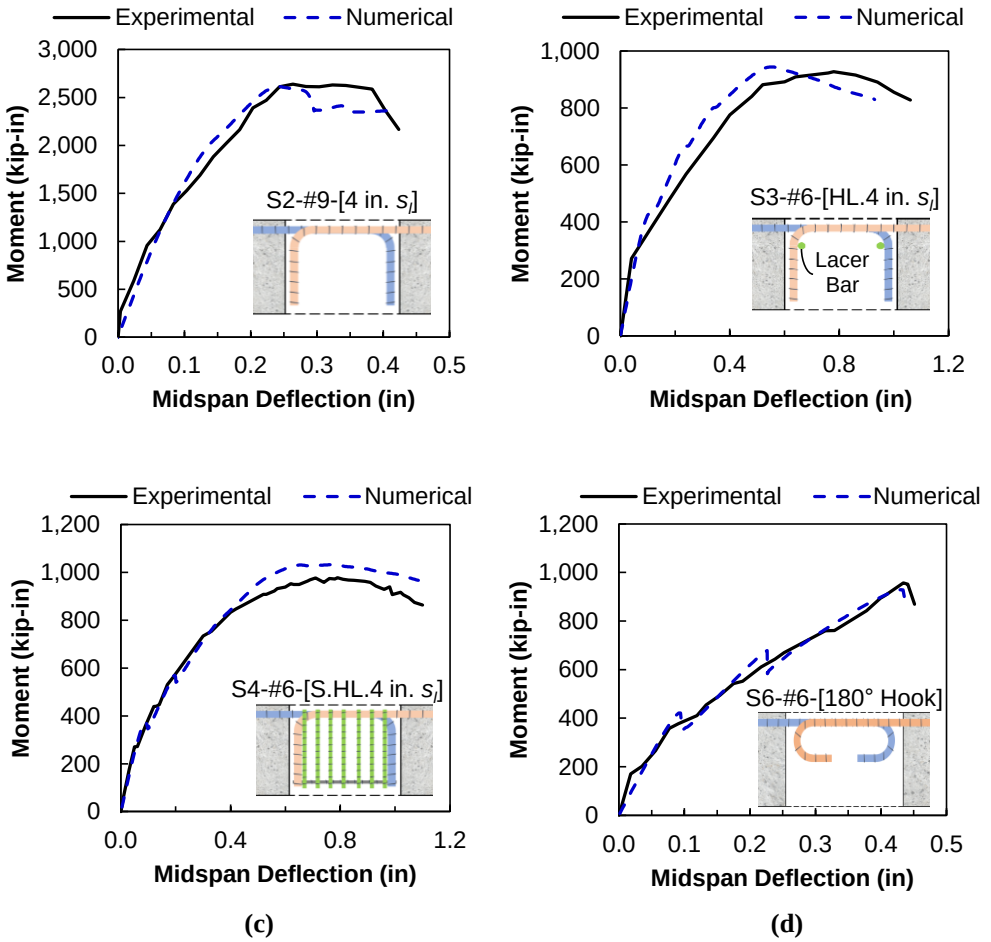

Figure 23. Comparison of Experimental and Numerical Results for Validation Beam-Splice Specimens: (a) S2-#9-[4 in s_l]; (b) S3-#6-[HL.4 in s_l]; (c) S4-#6-[S.HL.4 in s_l]; and (d) S6-#6-[180° Hook]

The numerical and experimental cracking patterns were similar, further validating the model approach. The numerical cracking patterns were inferred from the maximum principal strain contours and compared with observed cracking patterns in specimens S2-#9-[4 in s_l] and S4-#6-[S.HL.4 in s_l] (Figures 24 and 25). The maximum principal strain distributions in the models were similar to the experimental crack patterns, demonstrating that the models captured the damaged mechanisms of hooked bar lap splices.

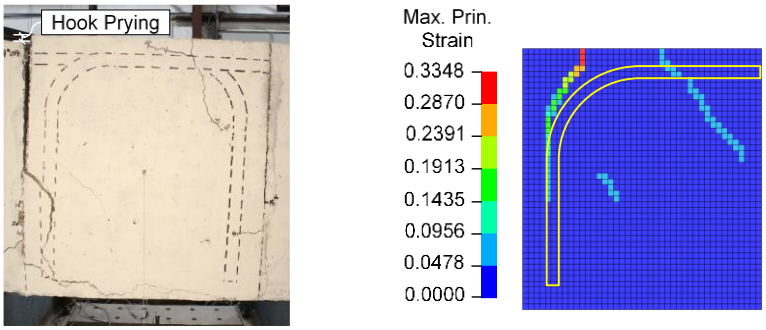

(a) **(b)**

Figure 24. Comparison of (a) Experimental Cracking Pattern and (b) Maximum Principal Strain Contour for Specimen S2-#9-[4 in s_l] not Containing Transverse Reinforcement

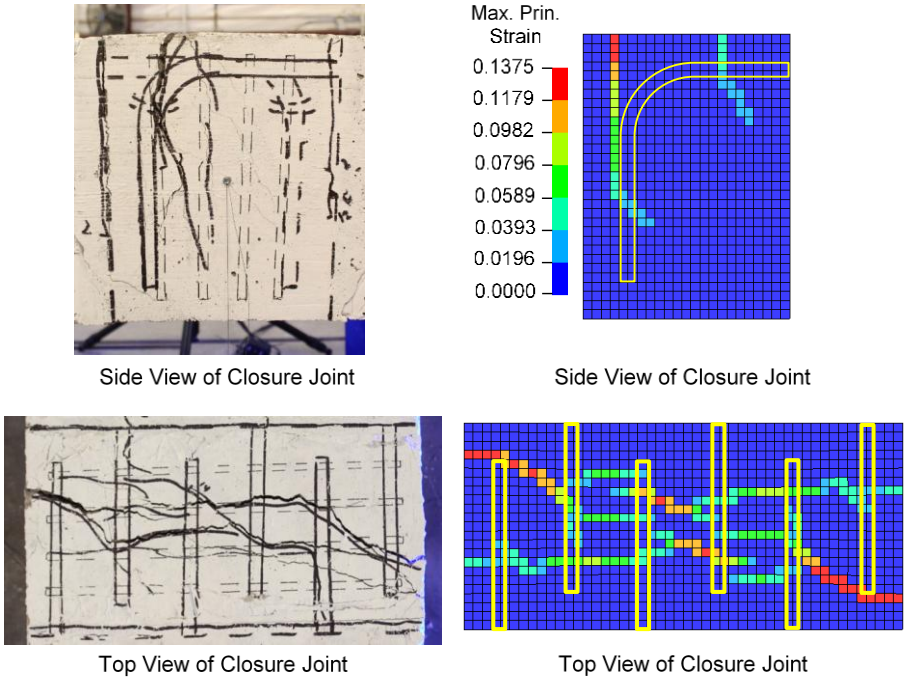

(a) **(b)**

Figure 25. Comparison of (a) Experimental Cracking Pattern and (b) Maximum Principal Strain Field for Specimen S4-#6-[S.HL.4 in s_l] Containing Transverse Reinforcement

Results of Finite Element Parametric Studies

Effect of Beam Height

Figure 26 shows the results of the parametric study examining the effect of beam depth on splice strength. The average bar stress f_s at peak capacity predicted by the finite element analysis was normalized by the yield stress f_y. Consistent with the findings from Test Series 10 (Table 3), the results show that the beam height did not substantially affect the strength of noncontact hooked bar lap splices. There was no clear trend between beam height and bar stress for the three specimens without transverse reinforcement in Figure 26a. The average bar stresses across all beam heights were within 5% of one another.

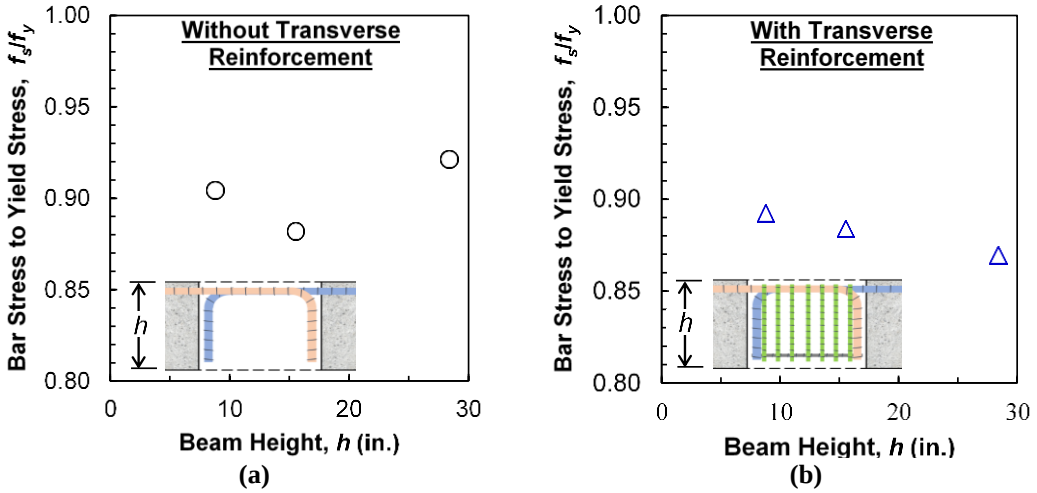

Figure 26. Results of Parametric Study of Beam Height for Lap Splices: (a) Without Transverse Reinforcement and (b) With Transverse Reinforcement

However, a negative correlation between beam height and bar stress was observed for the three specimens with transverse reinforcement in Figure 26b, although the average stresses of the specimens were within 4% of one another. Given the negligible effect of beam depth on splice strength, no large beam depth effect is believed to exist in hooked bar lap splices, unlike in beam-column joints. This result is consistent with the experimental data in Figure 19a.

Effect of Number of Lap Splices

Figure 27 presents the results of the parametric study examining the effect of the number of lap splices (i.e., one-half of all bars at the center of the splice region) on splice strength. The average bar stress f_s at peak capacity was normalized by the yield stress f_y and plotted against the number of lap splices of each beam. An increase in the number of lap splices n was found to increase splice strength. Whether or not transverse reinforcement was present, the results indicated a positive, linear correlation between the number of splices and the average splice strength. Increasing the number of lap splices increases the number of interior hooks while keeping the number of edge hooks constant. Because interior hooks carry greater force than edge hooks (Coleman, 2024), by increasing the number of splices, the average force carried by a hook increases, resulting in a higher average splice strength.

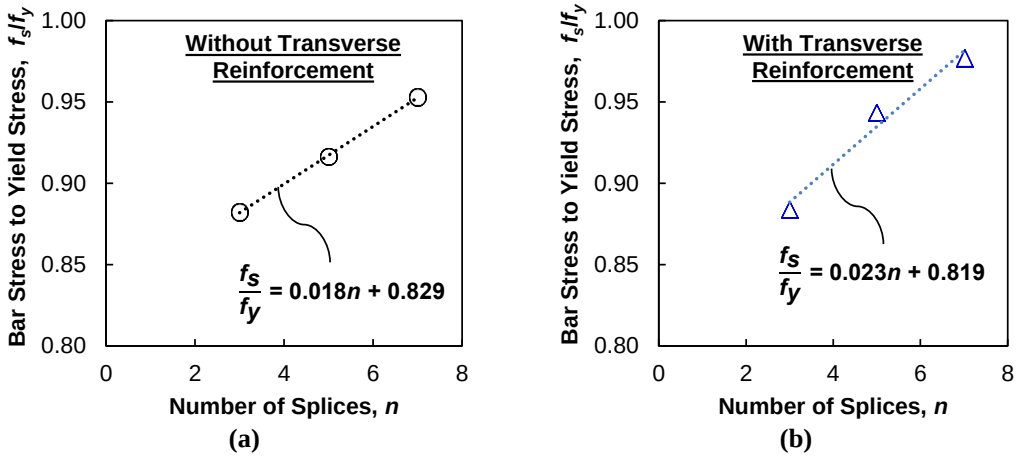

Figure 27. Results of Parametric Study of Number of Lap Splices: (a) Without Transverse Reinforcement and (b) With Transverse Reinforcement

Effect of 90° Hook Tail Length

Figure 28 gives the results of the parametric study investigating the effect of hook tail length on splice strength. The peak load P resisted by the beams before splice failure are plotted with their corresponding tail lengths l_{ext}. Decreasing the tail length of 90° hooks resulted in a reduction in splice strength. From Figure 28, each decrease in tail length from the standard hook ($12d_b$ tail) to that with no tail ($0d_b$) resulted in a decrease in peak beam strength. Therefore, shortening hook tails without prior analysis and testing is not recommended.

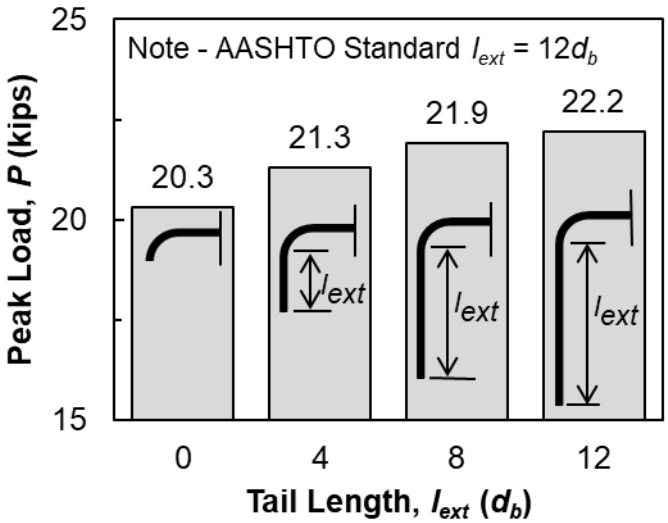

Figure 28. Results of Parametric Study Showing a Decrease in Splice Strength with Decreasing Tail Length of 90° Hooks. AASHTO = American Association of State Highway and Transportation Officials.

Effect of Lacer Bar Detailing

Figure 29 presents the results of the parametric study examining the effects of lacer bar detailing on the performance of noncontact hooked bar lap splices. From Figure 29, the

unconfined beam without lacer bar, or No Bar, was predicted to have the lowest strength and toughness, expressed as the area under the curve. The introduction of a straight No. 3 lacer bar, or Straight Bar (Figure 6a), into the splice resulted in an 8% increase in strength and somewhat improved toughness. Surprisingly, the use of a hooked lacer with the leg outside the lap length, or Hooked Outside (Figure 6c), had practically the same effect on the beam behavior of the hooked bars, or Hooked Inside, (Figure 6b). The hypothesis was that the hook would be more effective in anchoring the lacer bar to resist the transverse tension forces in Figure 12a. However, the positive effect of the hook appeared to have been offset by placing the leg of the lacer bar outside the lap length.

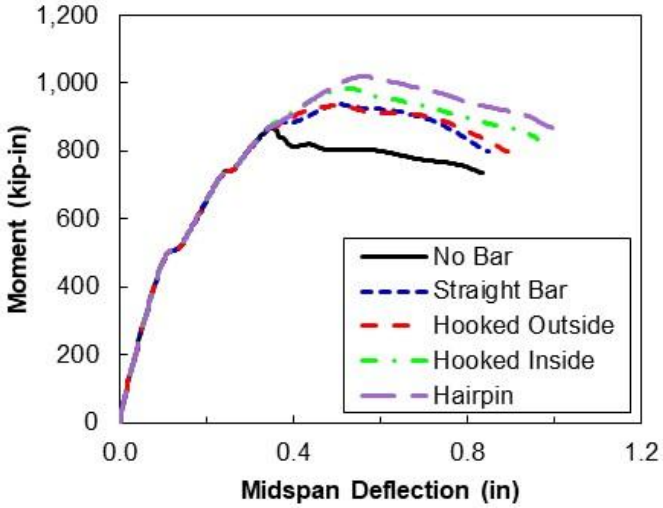

Figure 29. Moment-Deflection Plots for Parametric Study of Beams with Varying Lacer Bars. See Figure 6 for lacer bar details.

These results indicate that lacer bars should be placed in front of the lapped hooks to efficiently resist transverse tensile stresses due to anchorage. This practice is further supported by the fact that the hooked lacer bar with the leg placed inside the curvature of the hooks (Hooked Inside) resulted in a 13% increase in strength relative to the beam without transverse reinforcement.

Consistent with the experimental results presented previously in this report, the hairpin lacer, or Hairpin (Figure 6d), bar was most effective in increasing anchorage strength, as Figure 29 shows. Relative to the beam without transverse reinforcement, the beam with hairpin lacer bars exhibited 18% higher anchorage strength, a greater improvement in strength than any other lacer bar. The numerical results suggest that straight lacer bars should be avoided whenever possible. Although the difference in splice strength associated with each type of lacer bar was relatively minor (the hairpin bar increased the splice strength by 9% relative to the straight bar), hairpin lacer bars are more effective because they provide two legs of reinforcement to anchor edge hooks, which are susceptible to failure.

Based on the previously mentioned results, it is recommended that Article 3.6.2.2 of the AASHTO (2018) *LRFD Guide Specifications for Accelerated Bridge Construction* be amended to require using hairpin lacer bars that enclose edge hooks rather than the weaker straight bars.

Effect of Perpendicular Tie Location

The parametric study on the effect of perpendicular tie location revealed that positioning ties too close to the ends of the splice does not improve splice strength (Figure 30). As Figure 30b illustrates, ties at the splice ends develop strength levels comparable with those of similar hooked bar lap splices without transverse reinforcement. This finding is consistent with results from the parametric study on lacer bar detailing, which indicated that placing the leg of a hooked lacer bar outside the inner hook curvature is less effective than positioning it inside. However, this finding contrasts with the belief for straight bar lap splices that transverse reinforcement is most effective at the splice ends (Frosch et al., 2020) because bond stresses tend to be highest at the splice ends prior to bond failure (Tepfers, 1973).

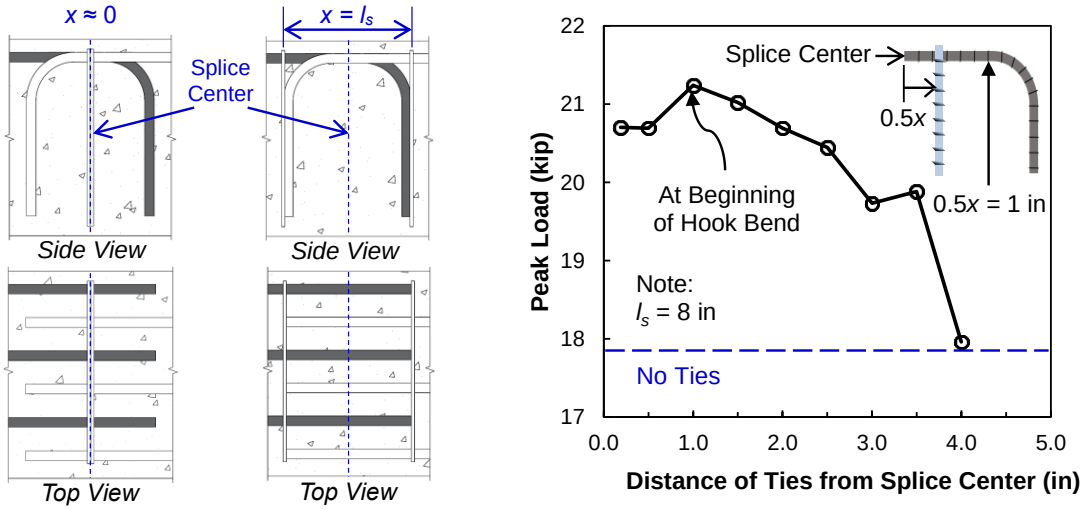

Figure 30. Effect of Perpendicular Tie Positions on Splice Strength: (a) Range of Tie Positions Considered and (b) Normalized Peak Beam Resistance as a Function of Tie Position

Two potential reasons are hypothesized for the diminished effectiveness of ties placed at the spliced ends. First, 35° anchorage cracks relative to the axis of a spliced bar could be observed at the hooked splice ends of some test specimens at failure, suggesting that ties at the splice ends cannot arrest the propagation of these cracks. Second, a perpendicular tie placed at the splice ends likely lacks the capacity to substantially improve the constitutive properties of the concrete inside the hook curvature because of clamping pressures, thereby resulting in little increase in anchorage strength.

This finding does not necessarily suggest that ties are inherently most effective near the center of the splice. Instead, the highest splice strength was achieved when ties were positioned at $0.25l_s$ from the splice center. This specific placement aligns closely with the location where the hook bend begins, suggesting that the most effective location for ties may be at the beginning of the hooked ends of the splice bars. To further substantiate this hypothesis, additional tests or simulations across a variety of splice lengths would be beneficial.

Based on these results, the researchers recommend placing the outermost perpendicular ties in front of the hook tails (i.e., not within $1d_b$ from the splice ends). Strategically distributing

multiple ties across the hook curvature could enhance the constitutive properties of the concrete within the hook. Distributing ties toward the center of the splice may also be helpful to improve splice strength, although future research may demonstrate that ties reinforcing the hooked ends of the splice rather than the splice center are more effective.

Effect of Parallel Tie Location

Figure 31 presents the results of the finite element simulation examining the stresses in parallel ties. Each tie is given an identification number in Figure 31. Tie No. 1 is the tie closest to the top of the hooks. Each subsequent tie is the next closest to the top of the hooks with tie No. 6 being the farthest away.

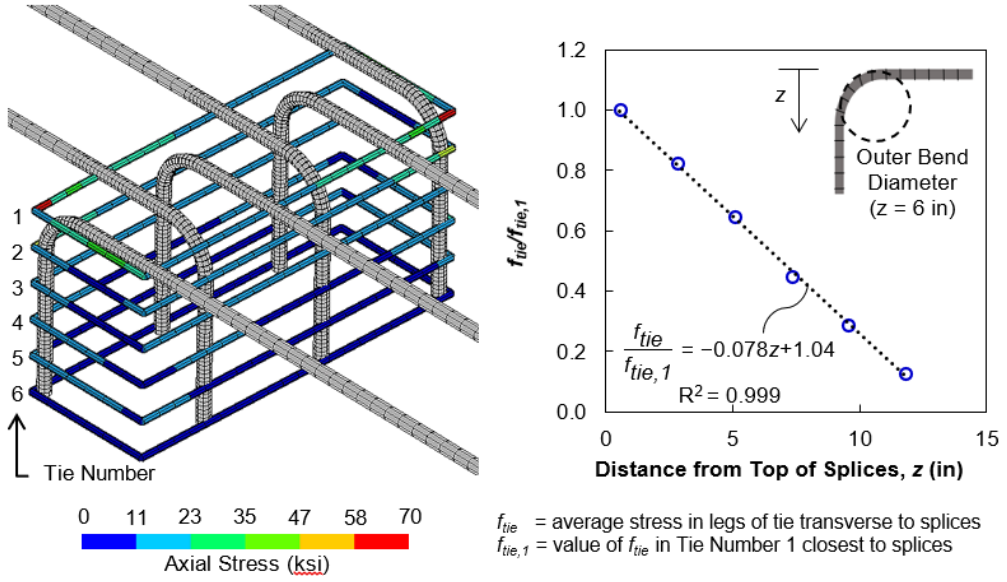

(a) **(b)**

Figure 31. Numerical Results of Beam with Parallel Ties at Peak Capacity: (a) Distribution of Stresses in Ties and (b) Average Tie Stress versus Distance from Lapped Bars

Several observations regarding the stresses in the parallel ties can be made from Figure 31. First, the average stress in the ties decreases with distance from the top of the hooks toward the hook tails. For example, tie No. 2 experiences less stress than tie No. 1, with the stress decreasing in ties farther from the top of the hooks. Second, the highest stresses in the parallel ties occur in the corners enclosing the edge hooks. This occurrence supports the idea that parallel ties resist transverse tension caused by splice eccentricity because the lateral force demand is greatest near the edge bars and decreases toward the interior of the beam. Lastly, the stress in most parallel ties remained well below yielding. Therefore, similar to straight bar lap splices (Azizinamini et al., 1995), transverse reinforcement in noncontact hooked bar lap splices is unlikely to yield before splice failure.

To determine which ties were most effective in improving splice strength, the average stress in the legs transverse to the spliced bars (the long legs of the ties in Figure 31b), denoted as f_{tie}, is plotted in Figure 31b as a function of the distance of the tie from the top of the splice z. The average stress in each tie was normalized by the average stress in tie No. 1, $f_{tie,1}$, to illustrate

the decay in tie effectiveness with increasing distance. The normalized tie stresses in Figure 31b show that an increase in distance (z) from the top of the hooks is highly correlated with a decrease in the average tie stress. For example, a parallel tie placed at the outer hook bend diameter (z = 6 inches) is expected to experience only 57% of the stress from tie No. 1 (z = 0.55 inch).

This finding is consistent with tests of hooked bars in beam-column joints by Ghimire et al. (2019) and Sperry et al. (2017) in that the parallel ties outside of the outer hook bend diameter are ineffective to increase anchorage strength. Based on the regression equation from Figure 31b, a tie placed at the outer hook bend diameter (z = 6 inches) is expected to experience only 57% of the stress from tie No. 1 (z = 0.55 inch). Thus, placing transverse reinforcement as close to the top of the hooks as possible to increase anchorage strength, thereby reducing required splice lengths, is most effective.

Future research could explore whether bundling or concentrating parallel ties within the hook bend radius provides greater resistance, or if uniformly distributing ties along the entire hook tail length, as in this study, is sufficient.

Effect of Interface Tensile Strength

Figure 32 shows the moment-deflection curves for the two finite element models, representing the monolithic and precracked interfaces for specimen S6-#6-[180° Hook]. The results confirm that the tensile strength of the interface has a negligible (practically zero) effect on the ultimate strength of the splice. Therefore, researchers concluded that the interface condition is not likely to affect the ultimate strength of noncontact hooked bar lap splices.

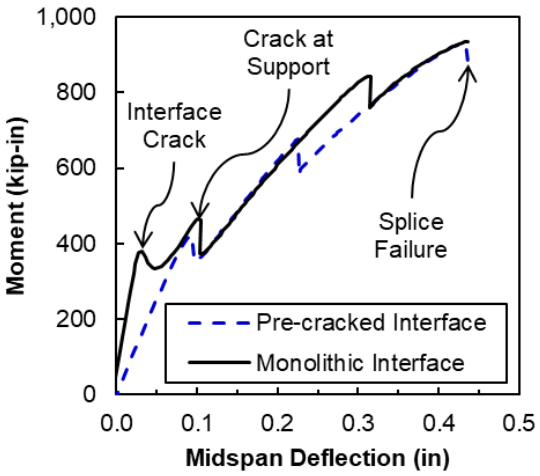

Figure 32. Moment-Deflection Curves from Parametric Study Illustrating the Negligible Effect of Interface Condition on the Ultimate Splice Strength

As Figure 32 shows, the monolithic interface condition results in higher initial stiffness compared with the precracked interface model. However, after cracking occurs at the interface, the stiffness of the two models becomes comparable. Both cases also exhibit localized drops in

resistance following interface cracking, caused by the formation of cracks near the supports and elsewhere in the beams.

Task 4: Design Equation for the Splice Length of Noncontact Hooked Reinforcing Bars

Descriptive Equation for the Strength of Hooked Bar Lap Splices

Regression analysis of the test results from Tables 2 through 4 produced the descriptive equation, Equation 1, which best predicts the strength of hooked bar lap splices, using kip-in units:

$$f_s^p = \frac{5.55 l_s^{0.67} f_{cm}^{0.33} \left(\frac{(0.1 c_{so} + 0.7 c_b)}{d_b} + K_{tr} \right)^{0.22}}{s_l^{0.033} d_b^{1.00}} \qquad \text{Equation 1}$$

where:

f_s^p = the predicted strength of a hooked bar lap splice (ksi).
l_s = the lap length of a hooked bar lap splice (in).
f_{cm} = the uniaxial concrete compressive strength (ksi).
c_{so} = the side cover (in).
c_b = the vertical cover (in).
d_b = the hooked bar diameter (in).
K_{tr} = $6.5NA_{tr1}$.
N = the number of legs of transverse reinforcement within one outer bend diameter from the top of the lapped bars, toward the hook tails.
A_{tr1} = the area of one leg of transverse reinforcement (in^2).
s_l = the inter-splice bar spacing (in).

Figure 33 shows example calculations to determine the number of transverse reinforcement legs N to consider in the K_{tr} calculation for each type of transverse reinforcement.

- The splice containing perpendicular ties has four ties, each with one leg transverse to the lapped hooks and positioned one outer bend diameter from the top of the lapped bars (N = 4). The vertical legs of the ties do not count toward the calculation of N. Thus, K_{tr} = $26A_{tr1}$.
- The splice with parallel ties has six ties. However, only three of those ties are within one outer bend diameter from the top of the lapped bars. Furthermore, each of the three ties within the hook bend diameter has two legs that are transverse to the lapped hooks. Therefore, six effective legs of transverse reinforcement are present, (N = 6) and K_{tr} = $39A_{tr1}$.
- The splice with hooked lacer bars has two bars, each of which has one leg transverse to the lapped bars (N = 2). Therefore, K_{tr} = $13A_{tr1}$. If hairpin lacer bars were used, four legs transverse to the lapped bars would be present, (N = 4) and K_{tr} = $26A_{tr1}$.

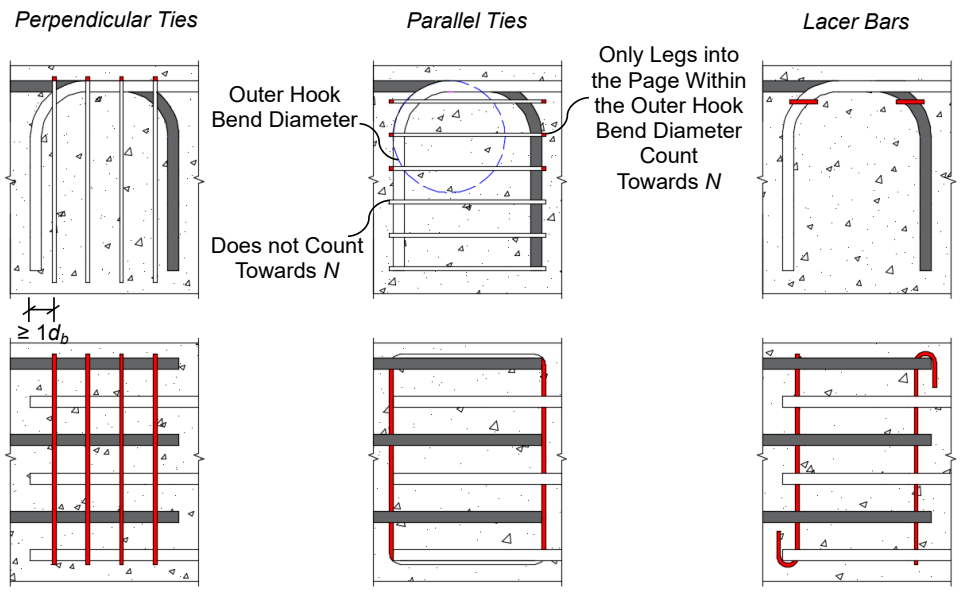

N = number of legs of transverse reinforcement in a plane parallel to the spliced bars and within one outer hook bend diameter from the top of the lapped bars, towards the hook tails
A_{tr1} = area of one leg of transverse reinforcement

Blue font designates reinforcement that counts towards *N*. Legs of reinforcement within the plane of the hook (top) do not count. Legs of reinforcement within a plane parallel to the splice (bottom) count.

Figure 33. Example Calculations to Determine the Number of Effective Transverse Reinforcement Legs *N* to Include in the Calculation of K_{tr}

Figure 34a compares the predicted stresses f_s^p calculated using Equation 1 to the experimental stresses f_s for all 58 tests in the database.

The average of all test-to-predicted stress ratios was 1.00, and COV was 5.3%, with minimum and maximum test-to-predicted stress ratios of 0.86 and 1.15, respectively, based on 58 observations. The descriptive equation predicts the stress at failure for noncontact hooked bar lap splices, equally with and without transverse reinforcement. Furthermore, the data clustered around the diagonal line in Figure 34a indicate that the descriptive equation accurately predicts the strength of noncontact hooked bar splices over the full range of experimental stresses.

To investigate whether the descriptive equation can consistently capture normal parameter changes, the slopes of the best-fit trendlines for the test-to-predicted stress ratios in Figures 34b through 34f were examined. These figures illustrate the test-to-predicted stress ratios as a function of splice length, concrete compressive strength, splice spacing, bar diameter, and the index of cover and transverse reinforcement. All slopes are nearly zero. In addition to the fact that the average test-to-predicted stress ratio was 1.00, this outcome indicates that the descriptive equation accurately captures the effect of each anchorage parameter on splice strength.

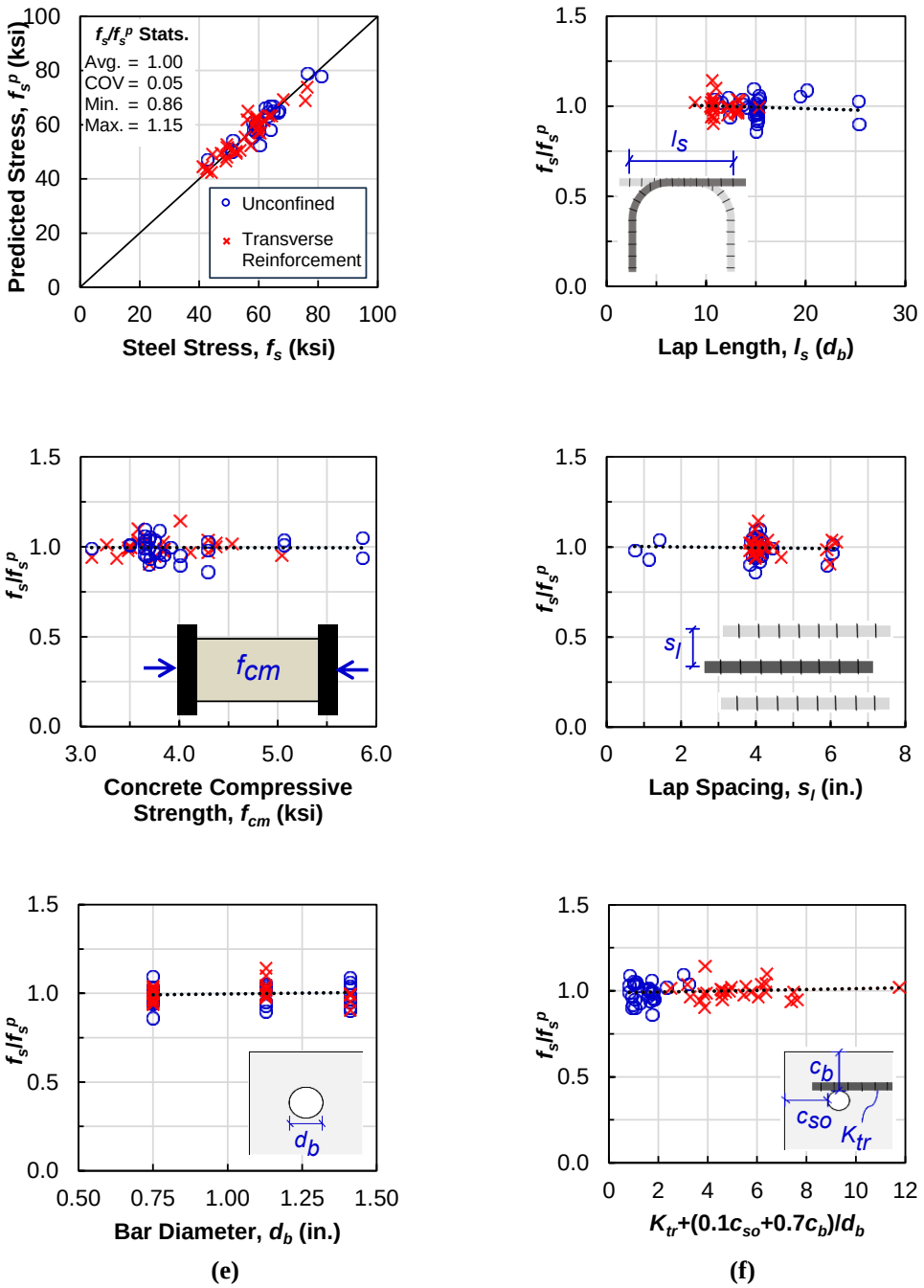

Figure 34. Performance of Descriptive Equation against: (a) Splice Strengths; (b) Splice Length; (c) Concrete Strength; (d) Splice Spacing; (e) Bar Diameter; (f) the Index of Cover and Transverse Reinforcement

The potential for predictive bias in the descriptive equation was further assessed by verifying that Equation 1 did not produce different results when applied to hooked bar lap splices with and without transverse reinforcement. A two-way t-test was conducted to determine if there was a statistically significant difference between the mean test-to-predicted stress ratios for the datasets of splices with and without transverse reinforcement. Using a 95% confidence level (i.e., a significance level of 0.05), the null hypothesis was that no statistically significant difference between the means of the two datasets existed. The p-value was 0.52, confirming no significant

difference in means. In other words, the descriptive equation produced similar results regardless of whether transverse reinforcement was provided in a lap splice.

The validity of the descriptive equation (Equation 1) was also evaluated by comparing the average test-to-predicted stress ratios for the groups of specimens with lacer bars, parallel transverse reinforcement, and perpendicular transverse reinforcement. Figure 35 shows that the maximum difference in the average test-to-predicted stress ratios between any two groups was only 1%, confirming that K_{tr}, which determines the influence of transverse reinforcement on splice strength in Equation 1, is accurate. However, given the number of samples containing lacer bars and parallel ties (four in both cases), future research is recommended to confirm this finding. Despite this finding, the results support the use of the K_{tr} definition, which accurately accounts for the effect of each type of transverse reinforcement on splice strength.

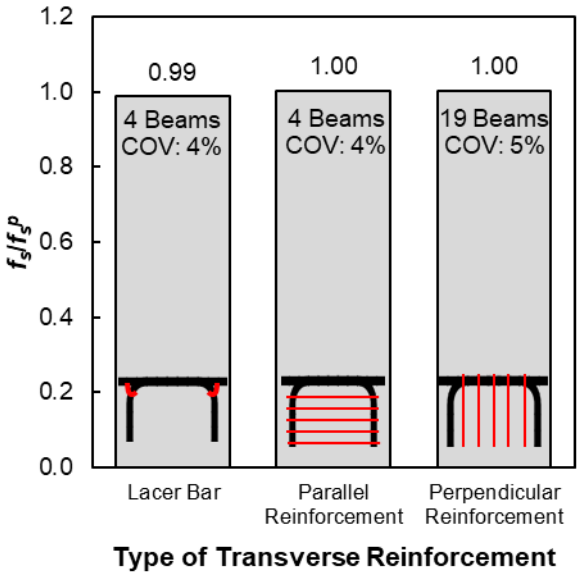

Figure 35. Uniform Accuracy of Descriptive Equation across All Types of Transverse Reinforcement. COV = coefficient of variation.

Discussion of Descriptive Equation

The following discussion describes the factors and coefficients derived from the regression analysis and used in Equation 1. The regression analysis produced weighting coefficients of 0.1 for the side with increased splice strength. For cases of equal side and vertical cover, classical bond theory would suggest an equal probability of a splitting failure in either direction due to uniform radial splitting forces generated by bar deformations wedging against the concrete. However, for a noncontact lap splice, the vertical cover is subjected not only to the splitting forces but also the transverse tensile forces caused by the splice eccentricity (Figure 12a). Thus, the vertical cover is more highly stressed relative to the side cover, justifying that the vertical cover is more highly correlated to splice strength than the side cover. Contrary to the provisions for noncontact lap splices of straight reinforcing bars in ACI Committee 318 (2019) and AASHTO (2020) *LRFD*, Equation 1 reveals that the anchorage strength of noncontact hooked bars decreases as the spacing of spliced bars s_l increases. For example, keeping all other factors constant, Equation 1 predicts that a No. 6 contact hooked bar lap splice is approximately

7% stronger than a noncontact splice with a 6-inch center-to-center spacing. This finding is consistent with previous test results in this report (e.g., Figure 15), in which an increase in splice spacing reduces anchorage strength because of an increase in the horizontal component of diagonal compression struts between hooks (see Figure 12a).

The power of 0.33 derived from the regression analysis for the concrete compressive strength is consistent with research by Coleman et al. (2023), who found that the power of 0.34 was most applicable for hooked bar anchorages in beam-column joints. Ajaam et al. (2018), who found that the power of 0.30 was most applicable for hooked bar anchorages in beam-column joints, further corroborated the validity of the power from the analysis. The researchers used the exponent 0.33 to present normalized test results from Task 2, discussed previously in this report.

Analogous to straight bar splices, the power of 0.22 on the index of cover and transverse reinforcement ($K_{tr} + (0.1c_{so} + 0.7c_b)/d_b$) suggests that incremental increases in cover or transverse reinforcement yield diminishing improvements to the anchorage strength of hooked bars.

Overall, the powers and coefficients determined through the regression analyses are consistent with the experimental test results, finite element analyses, and understanding of the behavior of hooked bar lap splices developed thus far.

Design Equation for the Strength of Hooked Bar Lap Splices

Although the descriptive Equation 1 was highly accurate in predicting the strength of hooked bar lap splices in this report, a design equation required further simplification and the introduction of a strength reduction factor.

Typically, a strength reduction factor for bond is established that produces a 5% fractile of test-to-calculated stresses less than 1.0 (International Federation for Structural Concrete, 2014; Lepage et al., 2020). The 5% fractile is approximately equivalent to a reliability index of 3.5 (Lepage et al., 2020), the minimum required reliability index for Risk Category II structural components exhibiting brittle failure modes (American Society of Civil Engineers, 2022). Although a strength reduction factor of 0.90 would produce a 5% fractile of test-to-calculated stresses less than 1.0, a lower factor of 0.75 was used because edge bars carry less tension than interior bars (Coleman, 2024). The 0.90 reduction factor, derived from bar stresses of moment-curvature analysis that assumed uniform tension across all hooks, needed to be adjusted to ensure that edge hooks would reach their design yield stress. Coleman (2024) observed that edge hooks might carry only 77% of the tension resisted by an interior hook at failure. Considering that most tests used to develop Equation 1 were from beams containing three pairs of splices, the failure stress in edge hooks was only about 84% of the moment-curvature stresses, which averages the stresses from the interior and edge hooks. Consequently, multiplying 0.90, which establishes the 5% fractile for average stresses, by 0.84, to ensure that edge hooks achieve the target average stress, yields a conservative strength reduction factor of approximately 0.75.

To simplify Equation 1 and produce a design equation, the cover term $(0.1c_{so} + 0.7c_b)$ was replaced with the minimum cover ($c_{min} = \min\{c_{so}, c_b\}$), and regression analysis was

conducted again, changing the leading constant from 5.55 to 5.40. Thus, the COV of this modified descriptive equation increased from 5 to 6%.

$$f_s^p = \frac{5.4 l_s^{0.67} f_{cm}^{0.33} \left(\frac{c_{min}}{d_b} + K_{tr}\right)^{0.22}}{s_l^{0.033} d_b^{1.00}} \quad \text{Equation 2}$$

Next, to determine the minimum required splice length of hooked bars, the modified descriptive expression was multiplied by the strength reduction factor (0.75), and splice strength f_s was replaced by yield strength f_y.

$$f_y = \frac{(0.75)5.4 l_s^{0.67} f_{cm}^{0.33} \left(\frac{c_{min}}{d_b} + K_{tr}\right)^{0.22}}{s_l^{0.033} d_b^{1.00}} \quad \text{Equation 3}$$

This resulting equation was rearranged to solve for the minimum required splice length as a function of the yield strength using kip-in units (Equation 4):

$$l_s = \left(\frac{f_y^{1.5} s_l^{0.05}}{8\sqrt{f_{cm}} \left(\frac{c_{min}}{d_b} + K_{tr}\right)^{0.33}} \right) d_b^{1.5} \quad \text{Equation 4}$$

When rearranged to solve for the splice strength as a function of lap length, Equation 4 results in an average test-to-calculated stress ratio of 1.33 and COV of 0.06. For splices without transverse reinforcement, the average test-to-calculated stress ratio was 1.32 (COV = 7%) based on 31 observations. For splices with transverse reinforcement, the average ratio was 1.35 (COV = 5%) based on 27 observations. As noted previously, the strength reduction factor (0.75) was selected to achieve an assumed reliability index of 3.5 against anchorage failure of the edge hooks. Supplemental files (see the link in the Abstract section) include recommended design provisions and commentary accompanying this design equation. These provisions and commentary reflect the range of parameters the researchers considered when developing Equation 4.

Figure 36 presents the steel strengths calculated using Equation 4 against corresponding experimental stresses, providing a visual assessment of the safety embedded in the design expression. The solid diagonal line in Figure 36 marks instances in which calculated and experimental strengths coincide. All observations fall below the diagonal line, indicating that the design equation allows for safely proportioning the minimum required lap length of hooked bar lap splices. The dashed line marks the center of the distribution of test-to-calculated stresses, including the strength reduction factor of 0.75. Because the individual cover terms were replaced with the minimum cover, the scatter in calculated stresses has increased relative to the scatter from Figure 34a.

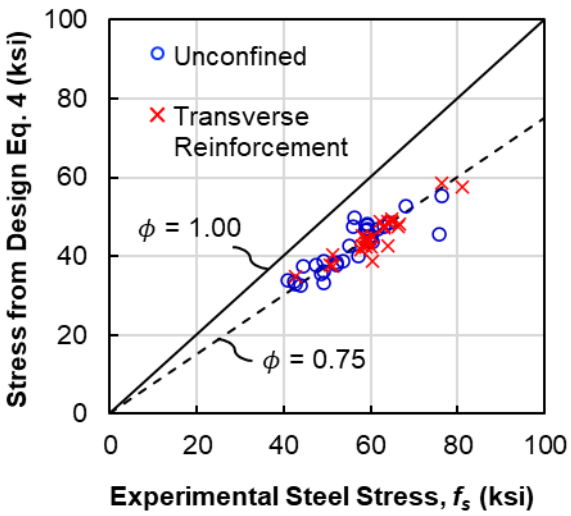

Figure 36. Calculated Splice Strengths Using Design Equation 4 for Hooked Bar Lap Splices Compared with Corresponding Experimental Strengths

Furthermore, the design equation is intended for use with Grade 80 or lower reinforcing bars no larger in size than No. 9. For bars of sizes No. 10 and No. 11, the equation is limited to Grade 60 or lower. The limit for the index of cover and transverse reinforcement ($K_{tr} + c_{min}/d_b$) is 8.0 because this study did not substantially examine higher levels of confinement.

Equation 4 can be applied to top-cast bars and bundled bars without having to increase the required splice length. This guidance is justified because top-cast bars and four-bar bundles did not demonstrate lower splice strengths compared with bottom-cast and nonbundled bars, respectively. Consistent with these findings, the average test-to-predicted stress ratios of the lap splices composed of top-cast bars and bundled bars calculated using the descriptive equation (Equation 1) were both 0.98, within 2% of the average test-to-predicted stress ratio. This deviation is negligible compared with the required increase in splice length reported by AASHTO (2020) *LRFD* for straight top-cast bars (30% increase) and four-bar bundles (33% increase). An important note is that the bar diameter d_b to use in Equation 4 for bundled bars should be the diameter of an equivalent bar with the combined cross-sectional area of all of the bundled bars instead of the diameter of the individual bars comprising the bundle.

Equation 4 should not be used for detailing hooked bar lap splices in scenarios with multiple layers of hooked reinforcement spliced at the same location. As demonstrated in Figure 18, two layers of hooked reinforcement reduce the stress that can develop in the spliced bars because of the group effect commonly observed in closely spaced embedded anchors. In other words, closely spaced hooked bars mobilize less concrete per hook than widely spaced bars, resulting in decreased resistance per bar. Thus, Equation 4, developed using only tests of beams containing one layer of reinforcement, may not be used to determine the required splice length when multiple layers of spliced hooks are used.

Furthermore, it is important to acknowledge that the design provisions developed in this research program were based solely on tests of monotonically loaded elements. Consequently,

the effects of fatigue and reverse cyclic loading on the required hooked bar lap length are unknown. Future research is recommended to address these knowledge gaps.

Design Examples

The design equation for the required lap length was developed based on the concrete compressive strengths measured from the beam tests f_{cm}. In practice, a minimum concrete compressive strength f_c' is specified and will be used instead for the design equation in the following examples.

Example 1: Noncontact Hooked Bar Lap Splice Length

Design the required splice length l_s for a single layer of Grade 60 No. 6 hooked bars with a bar spacing s_l of 3 inches, using 4 ksi concrete, and a minimum side and vertical cover c_{min} of 3 inches. Three-bar bundles of No. 6 bars are used. Four No. 4 ties, perpendicular to the spliced bars, are provided along the splice length. No ties are within $1d_b$ of the splice ends. The hooked bars can terminate in 90° hooks, 180° hooks, or U-bars. The choice of termination does not affect the results because this study demonstrated no apparent correlation between splice strength and hook shape.

The equivalent bar diameter, d_b, corresponding to the sectional area of bundled bars, is first determined. The area of a No. 6 bar is 0.44 inch^2. Therefore, the area, A_b, of a three-bar bundle of No. 6 bars is 1.32 inches^2. The equivalent bar diameter of the bundle is calculated using the formula for the cross-sectional area of a circle.

$$d_b = \sqrt{\frac{4A_b}{\pi}} = \sqrt{\frac{4(1.32\ \text{in}^2)}{\pi}} = 1.30\ \text{in}$$

The equivalent bar diameter is less than a No. 11 bar (1.41 inches). Therefore, the engineer may use the recommended design provisions in the supplemental files (see the link in the Abstract section).

K_{tr} is calculated using Equation 3.2b in the recommended design provisions. The result is four ties, each of which has one effective leg of reinforcement transverse to the lapped bars. Therefore, $N = 4$. The area of a No. 4 bar is 0.20 inch^2. Therefore, $A_{tr1} = 0.20$ inch^2.

$$K_{tr} = 6.5NA_{tr1} = 6.5(4)\left(0.20\ \text{in}^2\right) = 5.20$$

Next, the index of concrete cover and transverse reinforcement ($K_{tr} + c_{min}/d_b$) is calculated.

$$(K_{tr} + c_{min}/d_b) = (5.20 + 3\ \text{in} / 1.30\ \text{in}) = 7.50$$

The index of concrete cover and transverse reinforcement is less than the maximum value, which may be used to reduce the splice length (8.00).

All parameters can now be substituted into Equation 3.2a from the recommended design provisions to calculate the minimum required splice length for the hooked bars:

$$l_s = \left(\frac{{f_y}^{1.5} {s_l}^{0.05}}{8\sqrt{f_c'}\left(\frac{c_{min}}{d_b} + K_{tr}\right)^{0.33}} \right) {d_b}^{1.5}$$

$$l_s = \left(\frac{(60 \text{ ksi})^{1.5} (3 \text{ in})^{0.05}}{8\sqrt{4 \text{ ksi}}(7.5)^{0.33}} \right) (1.30 \text{ in})^{1.5} = 23 \text{ in}$$

Because the calculated splice length (23 inches) exceeds the minimum splice length of 8 inches, as section 3.1 of the recommended design provisions specifies, the required splice length for the hooked bars is 23 inches.

Example 2: Precast Bent Cap

This example illustrates the design of the minimum required splice length of hooked bars protruding from segments of a precast bent cap, which are joined together to accommodate a wide roadway. The design engineer attempted to position the lap splice as close to the inflection point of the moment diagram of the bent cap as practically feasible. The ends of the precast pieces are treated in accordance with the *Manual of the Structure and Bridge Division* (VDOT, 2022). This design example follows the recommended design provisions provided in the supplemental files (see the link in the Abstract section) and is intended to otherwise comply with AASHTO (2020) *LRFD*.

The cap width b is 72 inches. The concrete used in the closure joint connecting the precast segments shall have a specified 28-day compressive strength f_c' of 6 ksi using normal weight concrete. The reinforcing bars are corrosion-resistant and uncoated. The clear cover to the transverse reinforcement will be 1.5 inches. None of the hooked bars is bundled.

Based on the analysis of load demands and the cap configuration, the longitudinal tension reinforcement must nominally develop 900 kips. Assuming No. 11 bars (A_b = 1.56 in^2, d_b = 1.41 in) with Grade 60 steel (f_y = 60 ksi), 10 pairs of bars are required.

Next, the spacing of the No. 11 bars across the cap beam in a single layer must be determined. Assuming No. 5 bars (A_{tr1} = 0.31 in^2, d_{tr1} = 0.625 in) are used for the ties, the distance from the side of the beam to the center of the outermost spliced bar is calculated as the clear cover plus the tie diameter, plus the inside bend radius of the stirrup ($2d_b$):

Center of outer bar from side of beam = 1.5 in + 0.625 in + 2 × 0.625 in = 3.375 in.

Figure 37 shows this dimension. The center-to-center distance from the two outer-most bars is 65.25 inches. With 20 total bars and 19 spaces, the center-to-center spacing s_l is:

$$s_l = \frac{65.25 \text{ in}}{19 \text{ spaces}} = 3.43 \text{ in.}$$

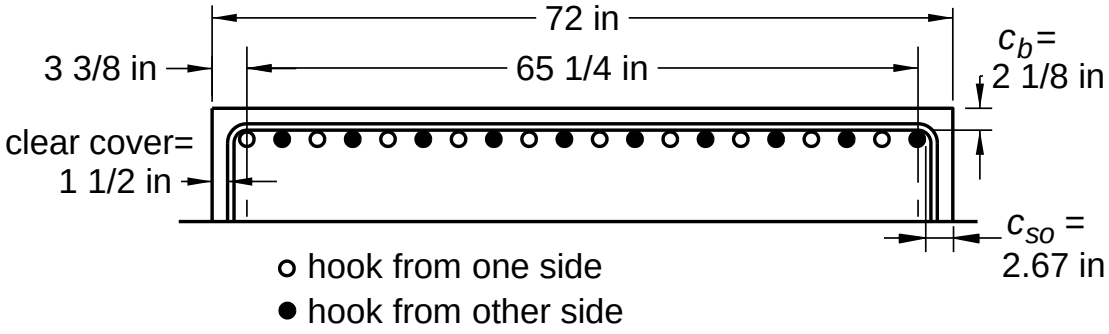

Figure 37. Cross Section of Pier Cap in Splice Region

Next, the tie diameter and spacing must be determined. Given the brittle nature of anchorage failures and the fact that large tension forces are developed in the plane of the splices, transverse reinforcement will be used. Assuming the ties are to be spaced at $4d_b$ (5.64 inches). Ties are spaced at $4d_b$ (5.64 inches), and the ties shall not be placed within $1d_b$ (1.41 inches) from the splice ends. It is assumed that five ties will be used.

To size the ties, the load transfer between the hooked bars is idealized using the strut-and-tie model in Figure 38. The analysis assumes that the concrete strut and node capacities will be sufficient as long as the minimum splice length is provided. It is assumed that all ties will contribute to resisting tensile forces.

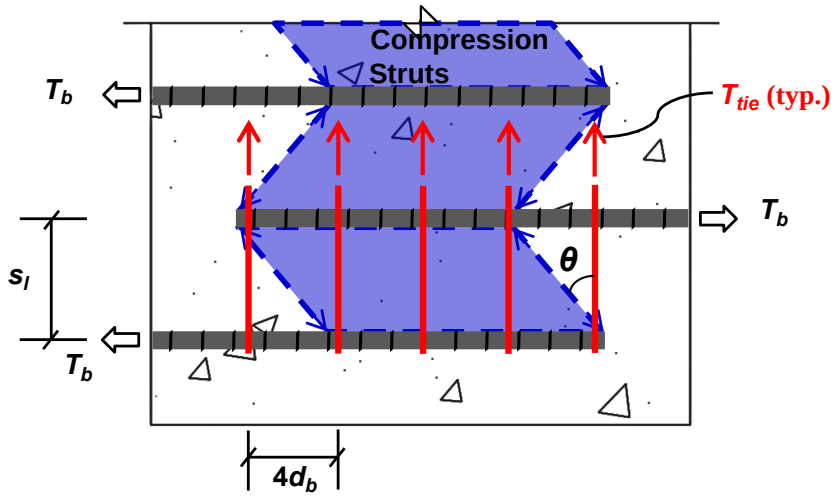

Figure 38. Idealized Load Path in Hooked Bar Lap Splice to Size Tension Ties

The compression strut angle θ is calculated as the arctangent of the tie spacing ($4d_b$ = 5.54 inches) divided by the splice spacing (s_l = 3.43 inches), resulting in θ = 58°. The tension in

each spliced bar ($T_b = A_b f_y$ = 94 kips) is assumed to generate equal tension in the four ties participating in force development. Because of the eccentricity between the spliced bars and the inclination of the struts, only four of the five ties are treated as developing tension in the strut-and-tie model. Therefore, the force in each tie is $T_{tie} = T_b / (4 \times \tan \theta)$ = 14.7 kips.

The required tie area, assuming Grade 60 reinforcement and a resistance factor of 0.90 (AASHTO [2020] *LRFD* Article 5.5.4.2), is 0.27 inch^2. Thus, the use of No. 5 bars (A_{tr1} = 0.31 inch^2) is satisfactory.

The required splice length of the noncontact hooked bars can now be calculated using the selected perpendicular tie reinforcement of five No. 5 ties distributed over the splice length. First, the index of transverse reinforcement K_{tr} is calculated using Equation 3.2b from the recommended design provisions (see the link for the supplemental files in the Abstract section) as follows:

$$K_{tr} = 6.5NA_{tr1} = 6.5(5)\left(0.31 \text{ in}^2\right) = 10$$

where A_{tr1} is the area of one leg of tie reinforcement and N is the number of legs of tie reinforcement within the splice length minus $1d_b$ from either splice end. The index of concrete cover and transverse reinforcement is then calculated:

$$\frac{c_{min}}{d_b} + K_{tr} = \frac{2.125 \text{ in}}{1.41 \text{ in}} + 10 = 11.5$$

where c_{min} is the minimum of the side and vertical covers (2.125 inches) to the spliced bars.

In accordance with section 3.2 of the recommended design provisions, the maximum value of the confinement term is 8.0, which will be used hereinafter. The minimum required splice length in accordance with Equation 3.2b of the recommended design provisions is:

$$l_s = \left(\frac{f_y^{1.5} s_l^{0.05}}{8\sqrt{f_c'}\left(\frac{c_{min}}{d_b} + K_{tr}\right)^{0.33}} \right) d_b^{1.5}$$

$$l_s = \left(\frac{(60 \text{ ksi})^{1.5} (3.43 \text{ in})^{0.05}}{8\sqrt{6 \text{ ksi}}(8)^{0.33}} \right) (1.41 \text{ in})^{1.5} = 21 \text{ in.}$$

The required splice length is 21 inches, which exceeds the minimum value of 8 inches. The total length available to space the ties is the lap length minus $1d_b$ from either end of the splice—i.e., 21 inches – $2d_b$ = 18.18 inches—resulting in a center-to-center spacing of 4.55 inches ($3.2d_b$) for the five ties, which is smaller than the initial design choice of 5.64 inches ($4.0d_b$). Despite the reduced tie spacing, the ties approximately have sufficient tensile capacity, per the strut-and-tie model of Figure 38. To allow for consolidation of concrete beyond the ends of the lapped reinforcement and construction tolerances, an extra 2 inches of joint length will be

provided on either end of the lap. Thus, the final closure-joint width using the hooked bar lap splices is 25 inches (Figure 39).

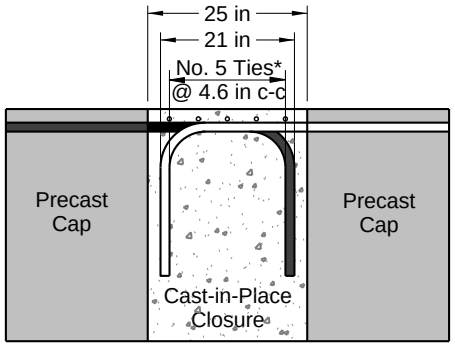

* vertical legs of ties are not shown for clarity

Figure 39. Final Design of Noncontact Hooked Bar Lap Splices in Precast Bent Cap

An equivalent straight bar lap splice for No. 11 Grade 60 top-cast bars, calculated according to AASHTO (2020) *LRFD*, is 56 inches, which is 2.7 times the splice length of the equivalent noncontact hooked bar lap splice.

CONCLUSIONS

- *Tension forces can be transferred over shorter distances if noncontact hooked bar lap splices are used in place of straight bar lap splices.*

- *Noncontact hooked bar lap splices transfer force through inclined compression struts spanning between the bars.* These struts induce a tension field perpendicular to the lapped bars. For unconfined lap splices, failure may occur because of rupturing of this tension field, causing the rigid-body displacement of a mass of concrete surrounding the edge hooks outward from the beam. This failure mode can be prevented by providing transverse reinforcement.

- *Transverse reinforcement in the splice region, in the form of ties or lacer bars, or both, resists the tension forces caused by eccentricity of the spliced bars, changing the failure mode to concrete crushing within the hook radius.* This positive effect can be characterized by a unified index of transverse reinforcement K_{tr}, which is applicable for lacer bars and configurations of parallel or perpendicular ties. For beams, perpendicular ties may generally be the most practical type of transverse reinforcement, because they can be used to reduce splice lengths and enhance shear resistance.

- *Lacer bars, parallel ties, and perpendicular ties are all effective in increasing splice strength.* However, various configurations and details of each type of transverse reinforcement are more effective than others. Hairpin lacer bars (i.e., bars with two legs transverse to the lapped reinforcement) enclosing each edge hook are the most effective type of lacer bar to increase anchorage strength. Parallel ties closest to the lapped bars are most

effective for improving splice strength. Perpendicular ties within $1d_b$ of the splice ends are ineffective to improve splice strength.

- *Increases in the following parameters result in increased splice strength: splice length, concrete compressive strength, cover, and the amount of transverse reinforcement.*

- *Increases in bar size, splice spacing, or the number of layers of spliced hooks result in reduced splice strength.*

- *A 1% dosage of steel fibers can substantially improve the strength and toughness of noncontact hooked bar lap splices.* However, future tests considering a wider range of fiber dosages and beam properties are required to confidently establish a reduction factor to the required splice length when using steel fibers.

- *Bar bundling or the top-cast effect does not affect the strength of hooked bar lap splices.* Thus, bundled or top-cast hooked bar lap splices can be used without a required increase in splice length. The diameter corresponding to the cross-sectional area of the bundle should be used when calculating the required splice length.

- *The design equation for the required splice length of noncontact hooked bars that was developed as a part of this research can ensure that all spliced noncontact hooks achieve their yield stress under ultimate factored loading*. This equation is believed to be superior to the design approach in the AASHTO (2018) *LRFD Guide to Accelerated Bridge Construction*, which was largely based on tests of small-diameter, hooked bars that did not fail in a manner related to anchorage.

RECOMMENDATIONS

1. *VDOT's Structure and Bridge Division should consider adopting the design provisions and commentary regarding the minimum required splice length of hooked bars in this report's supplemental files (see the link in the Abstract section).*

2. *When possible, engineers in VDOT's Structure and Bridge Division should opt for a greater number of small bars instead of a smaller number of large bars when detailing splices to minimize the required splice length.*

3. *When engineers design bundled hooked bar lap splices, VDOT's Structure and Bridge Division should require only the consideration of the combined cross-section of the bundle, not the number of bars in the bundle.* For this research, the maximum sectional area of a bundle should be limited to 1.56 inches^2, the area of a No. 11 bar. Likewise, the Structure and Bridge Division should encourage ACI Committee 318 (2019) and AASHTO (2020) *LRFD* to adopt the combined cross-sectional area approach.

4. *VDOT's Structure and Bridge Division should require the outermost perpendicular ties be placed in front of the hook tails (i.e., not within $1d_b$ from the splice ends).* Strategically

distributing multiple ties across the hook curvature could enhance the constitutive properties of the concrete within the hook. Distributing ties toward the center of the splice may also be helpful to improve splice strength.

5. *VDOT's Structure and Bridge Division should encourage AASHTO to amend Article 3.6.2.2 of the AASHTO (2018) LRFD Guide Specifications for Accelerated Bridge Construction.* AASHTO might consider adopting design guidance from this research (see the link for the supplemental files in the Abstract section) as an alternative design approach. In addition, AASHTO should consider requiring that hairpin lacer bars be used in noncontact hooked bar lap splices in place of weaker straight bars within the hook curvature.

6. *VDOT's Structure and Bridge Division and the Virginia Transportation Research Council should consider additional research to further refine the proposed design guidance and remove some of the limitations applied to the design equation*. This research could include (1) validating the design approach for noncontact hooked bar lap splices through full-scale tests on bent caps to address possible scaling effects, (2) further validation of large-scale tests with lacer bars and parallel ties to compare test-to-predicted stress ratios with the tests containing perpendicular transverse ties, (3) studying the performance of multiple layers of hooked bars to understand the reduction in achievable bar stress for splices with and without transverse reinforcement, (4) assessing the effect of service-level shear and fatigue loads on splice strength and durability, (5) investigating the positive effects of steel fibers on the anchorage strength of hooked bars over a broad range of design parameters to justify a reduction in required splice length, (6) experimentally confirming that interface treatments (e.g., shear keys) do not significantly affect splice strength, (7) exploring the use of higher strength concrete or high-performance concrete to improve splice strength and reduce required splice lengths, and (8) experimentally studying No. 11 hooked bar lap splices that develop at least 80 ksi of stress, such that proposed design guidance can be extended to include Grade 80 No. 11 bars.

IMPLEMENTATION AND BENEFITS

Researchers and the technical review panel (listed in the Acknowledgments) for the project collaborate to craft a plan to implement the study recommendations and to determine the benefits of doing so. This process is to ensure that the implementation plan is developed and approved with the participation and support of those involved with VDOT operations. The implementation plan and the accompanying benefits are provided here.

Implementation

Regarding Recommendations 1 through 4, VDOT's Structure and Bridge Division will incorporate the recommended design guidance into the VDOT (2022) Manual of the Structure and Bridge Division by the end of January 2027.

Regarding Recommendation 5, appropriate personnel from VDOT's Structure and Bridge Division will bring it to the chair of the Construction Technical Committee within

AASHTO's Committee on Bridges and Structures at the committee's next annual meeting in June 2026.

Regarding Recommendation 6, the Virginia Transportation Research Council will propose a new research project that incorporates the tasks as outlined in the recommendation. This proposal will be put forth to the Bridge Research Advisory Committee for their consideration of new research projects at their 2026 fall meeting.

Benefits

The benefits of implementing Recommendation 1 are that the proposed design equation and code guidance will ease the connection of structural components by using shorter splice lengths than what is achievable through straight bars. Furthermore, the design provisions have been statistically calibrated to achieve a high level of safety, preventing splice failures and allowing structural elements to achieve their intended level of strength and deformability. The proposed equation opens more opportunities for phased construction. Using shorter lap lengths can increase the number of girders or alter their locations on pier caps. These changes could open up additional driving lanes to traffic at the end of the first phase, thus reducing traffic congestion while the subsequent phase is constructed.

An even larger benefit could be gained through accelerated bridge construction (ABC). Although ABC tends to require higher upfront, direct costs, this construction technique can bring greater savings through shortened project delivery times and improved work-zone safety (FHWA, 2017; Knife River Prestress, Inc., 2025). Currently, only occasional bridge projects are built in Virginia using ABC. Using noncontact lap splice bars instead of grouted couplers with shear keys could make ABC feasible for more bridge components. For example, the Northern Virginia District completed the one known project with precast concrete footings in 2023. Although the district is still assessing the total cost savings for the project due to the contractor's performance, deploying the noncontact lap splice connection for more components, such as piers, breast walls, and wing walls (see the link provided in the report abstract), could reduce the overall project costs in the future.

Looking at VDOT's database inventory of bridges in the Northern Virginia District because of its heavily urban population, where ABC could be most beneficial, the average detour length for any given bridge is 12.6 miles. Assuming an average speed of 45 mph along that route, that equates to 16.8 minutes of extra travel time. Also, according to the database, the mean average daily traffic for bridges in this district is 19,666 vehicles per day, with the average truck percentage being 2.6%. Thus, the average bridge carries 19,155 cars and 511 trucks each day. According to Schrank et al. (2024), the unit congestion cost for a car was $23.12 per hour, and the unit congestion cost for a truck was $64.68 per hour in 2022 dollars. Adjusting for inflation, those costs in 2025 dollars are $0.43 and $1.21 per minute for cars and trucks, respectively. Therefore, the estimated daily cost to the traveling public for routing around a bridge closure is $191,300. One bridge in New Hampshire required only 3 days to build the substructure using prefabricated elements compared with what was estimated to take 2 months using conventional construction methods (FHWA, 2017). Therefore, the shortened duration using ABC for a similar

structure in Northern Virginia could be worth $8.5 million. Note that the net benefit will be smaller after taking the direct cost of accelerated construction into account.

Implementing Recommendations 2 through 4 will essentially maximize the design efficiency following the implementation of Recommendation 1. Using a greater number of smaller bars in splices, within constructability tolerances, can reduce the splice lengths to the greatest extent.

Although implementing Recommendation 5 does not directly benefit VDOT, implementation would improve the ABC community at large. Furthermore, engineers working on projects for other DOTs could become more familiar with best practices that could be incorporated into the designs that those engineers develop for VDOT projects.

The benefit of Recommendation 6 is to further expand the current research to explore the performance of alternative splice configurations and validate their effectiveness in different structural scenarios.

ACKNOWLEDGMENTS

The authors would like to thank the following people who served on the technical review panel for this study: Mr. Andrew M. Zickler (project champion), P.E., Complex and Bridge Support, Structure and Bridge Division; Mrs. Annette F. Adams, P.E., District Bridge Engineer, Fredericksburg District Structure and Bridge; Ms. Virginia J. Epperly, P.E., Design Team Leader, Richmond District Structure and Bridge; and Mr. Bruce G. Shepard, P.E., Engineering Program Manager, Structure and Bridge Division. The authors also gratefully acknowledge the assistance of Brett Farmer, David Mokarem, and Garrett Blankenship at the Thomas M. Murray Structural Engineering Laboratory at Virginia Tech. The authors are further appreciative of Ioannis Koutromanos for his assistance in conducting the finite element analyses of this study.

REFERENCES

Ajaam, A., Darwin, D., and O'Reilly, M. *Anchorage Strength of Reinforcing Bars with Standard Hooks*. SM Report No. 125. The University of Kansas, Lawrence, KS, 2017.

Ajaam, A., Yasso, S., Darwin, D., O'Reilly, M., and Sperry, J. Anchorage Strength of Closely Spaced Hooked Bars. *ACI Structural Journal*, Vol. 115, No. 4, July 2018, pp. 1143–1152.

American Association of State Highway and Transportation Officials. *LRFD Guide Specifications for Accelerated Bridge Construction*, 1st edition. Washington, DC, 2018.

American Association of State Highway and Transportation Officials. *LRFD Bridge Design Specifications*, 9th edition. Washington, DC, 2020.

American Concrete Institute Committee 318. *Building Code Requirements for Structural Concrete Standard (ACI 318-19) and Commentary (ACI 318R-19).* American Concrete Institute, Farmington Hills, MI, 2019.

American Concrete Institute Committee 408. *Bond and Development of Straight Reinforcing Bars in Tension.* American Concrete Institute, Farmington Hills, MI, 2012.

American Society of Civil Engineers. *Minimum Design Loads and Associated Criteria for Buildings and Other Structures*. ASCE Standard 7-22. Reston, VA, 2022.

ASTM International. *Standard Test Method for Static Modulus of Elasticity and Poisson's Ratio of Concrete in Compression*. ASTM C469-14. West Conshohocken, PA, 2014.

ASTM International. *Standard Test Method for Splitting Tensile Strength of Cylindrical Concrete Specimens*. ASTM C496-17. West Conshohocken, PA, 2017.

ASTM International. *Standard Test Method for Compressive Strength of Cylindrical Concrete Specimens*. ASTM C39-20. West Conshohocken, PA, 2020.

ASTM International. *Standard Test Methods and Definitions for Mechanical Testing of Steel Products*. ASTM A370-22. West Conshohocken, PA, 2022.

Au, A., Lam, C., and Tharmabala, B. Investigation of Closure Strip Details for Connecting Prefabricated Deck Systems. *PCI Journal*, Vol. 56, No. 3, June 2011, pp. 75–93.

Azizinamini, A., Chisala, M., and Ghosh, S.K. Tension Development Length of Reinforcing Bars Embedded in High-Strength Concrete. *Engineering Structures*, Vol. 17, No. 7, 1995, pp. 512–522.

Bashandy, T.R. Evaluation of Bundled Bar Lap Splices. *ACI Structural Journal*, Vol. 106, No. 2, March 2009, pp. 215–221.

Brown, M. *Alternative Reinforcing Strategies for Noncontact Hooked Bar Lap Splices*. Master's thesis. Virginia Polytechnic Institute and State University, Blacksburg, VA, 2024.

Brush, N.C. *Connection of Modular Steel Beam Precast Slab Units with Cast-in-Place Closure Pour Slabs*. Master's thesis. Texas A&M University, College Station, TX, 2004.

Cairns, J. Lap Splices of Bars in Bundles. *ACI Structural Journal*, Vol. 110, No. 2, March 2013, pp. 183–192.

Canbay, E., and Frosch, R.J. Bond Strength of Lap-Spliced Bars. *ACI Structural Journal*, Vol. 102, No. 4, July 2005, pp. 605–614.

Chamberlin, S.J. Spacing of Spliced Bars in Beams. *ACI Journal Proceedings*, Vol. 54, No. 2, February 1958, pp. 689–697.

Chinn, J., Ferguson, P.M., and Thompson, J.N. Lapped Splices in Reinforced Concrete Beams. *ACI Journal Proceedings*, Vol. 52, No. 10, October 1955, pp. 201–213.

Coleman, Z.W. *Hooked Bar Anchorages and Their Use in Noncontact Lap Splices*. Ph.D. dissertation. Virginia Tech, Blacksburg, VA, 2024.

Coleman, Z.W., Jacques, E., and Roberts-Wollmann, C. Effect of Beam Depth on the Anchorage Strength of Hooked and Headed Bars. *ACI Structural Journal*, Vol. 120, No. 3, May 2023, pp. 197–206.

Coleman, Z.W., Jacques, E., and Roberts-Wollmann, C. State of Practice and Design Examples for the Use of Noncontact Hooked Bar Lap Splices in Accelerated Bridge Construction. *Journal of Structural Design and Construction Practice*, Vol. 30, No. 3, August 2025a.

Coleman, Z.W., Koutromanos, I., Jacques, E., and Roberts-Wollmann, C. Finite Element Analysis of Noncontact Hooked Bar Lap Splices in Precast Concrete Connections. *Engineering Structures*, Vol. 326, March 2025b.

Darwin, D., and Graham, E.K. Effect of Deformation Height and Spacing on Bond Strength of Reinforcing Bars. *ACI Structural Journal*, Vol. 90, No. 6, November 1993, pp. 646–657.

Darwin, D., Zuo, J., Tholen, M.L., and Idun, E.K. *Development Length Criteria for Conventional and High Relative Rib Area Reinforcing Bars*. SL Report 95-4. The University of Kansas, Lawrence, KS, 1995.

Dragosavić, M., van den Beukel, A., and Gijsbers, F.B.J. Loop Connections Between Precast Concrete Components Loaded in Bending. *Heron Journal*, Vol. 20, No. 3, 1975, pp. 1–34.

Eligehausen, R., Popov, E.P., and Bertero, V.V. *Local Bond Stress-Slip Relationships of Deformed Bars Under Generalized Excitations*. UCB/EERC-83/23. University of California, Berkeley, CA, 1982.

Federal Highway Administration. Prefabricated Bridge Elements and Systems Cost Study: Accelerated Bridge Construction Success Stories, 2017. https://www.fhwa.dot.gov/bridge/prefab/successstories/091104/02.cfm. Accessed May 29, 2025.

French, C.E., Shield, C., Klaseus, D., Smith, M., Eriksson, W., Ma, Z., and Zhu, P. *Cast-in-place Concrete Connections for Precast Deck Systems*. NCHRP Web-Only Document 173. Transportation Research Board, Washington, DC, 2011.

Frosch, R.J., Fleet, E.T., and Glucksman, R. *Development and Splice Lengths for High-Strength Reinforcement, Volume I: General Bar Development*. Research Grant No. 02-17. Charles Pankow Foundation, McLean, VA, 2020.

Ghimire, K.P., Shao, Y., Darwin, D., and O'Reilly, M. Conventional and High-Strength Headed Bars—Part 2: Data Analysis. *ACI Structural Journal*, Vol. 116, No. 3, 2019, pp. 265–272.

Hamad, B.S., and Mansour, M. Bond Strength of Noncontact Tension Lap Splices. *ACI Structural Journal*, Vol. 93, No. 3, May 1996, pp. 316–326.

Harajli, M.H., and Salloukh, K.A. Effect of Fibers on Development/Splice Strength of Reinforcing Bars in Tension. *ACI Materials Journal*, Vol. 94, No. 4, July 1997, pp. 317–324.

Hognestad, E. A *Study of Bending and Axial Load in Reinforced Concrete Members*. Bulletin Series No. 399. University of Illinois Engineering Experiment Station, Urbana, IL, 1951.

Hwang, H., Yang, F., and Ma, G. Effect of Noncontact Lap Splices in Reinforced Concrete Beams. *ACI Structural Journal*, Vol. 119, No. 2, March 2022, pp. 3–18.

International Federation for Structural Concrete. *fib Model Code for Concrete Structures 2010*. Ernst & Sohn, Berlin, Germany, 2013.

International Federation for Structural Concrete. *Bond and Anchorage of Embedded Reinforcement: Background to the fib Model Code for Concrete Structures 2010*. Bulletin 72. International Federation for Structural Concrete, Lausanne, Switzerland, 2014.

Jahromi, A.J., and Azizinamini, A. *Investigation of Longitudinal Closure Joint Using 90° Hooked Bars in Accelerated Bridge Construction*. ABC-UTC-2013-C1-FIU05-Final. Florida International University, Miami, FL, 2019.

Jirsa, J.O., and Breen, J.E. *Influence of Casting Position and Shear on Development and Splice Length—Design Recommendations*. Research Report 242-3F. Texas State Department of Highways and Public Transportation, Austin, TX, 1981.

Jirsa, J.O., Chen, W., Grants, D.B., and Elizondo, R. *Development of Bundled Reinforcing Steel*. Research Report 1363-2F. Center for Transportation Research, The University of Texas at Austin, Austin, TX, 1995.

Joergensen, H.B., and Hoang, L.C. Strength of Loop Connections Between Precast Bridge Decks Loaded in Combined Tension and Bending. *Structural Engineering International*, Vol. 25, No. 1, February 2015, pp. 71–80.

Johnson, L.A., and Jirsa, J.O. *The Influence of Short Embedment and Close Spacing on the Strength of Hooked Bar Anchorages*. PMFSEL Report No. 81-2. The University of Texas at Austin, Austin, TX, 1981.

Kim, S.H., and Koutromanos, I. Constitutive Model for Reinforcing Steel Under Cyclic Loading. *Journal of Structural Engineering*, Vol. 142, No. 12, July 2016, pp. 1–14.

Knife River Prestress, Inc. Bridge Substructure, 2025. https://www.kniferiverprestress.com/products/bridge-substructure/. Accessed May 29, 2025.

Koutromanos, I., and Farhadi, M. *FE-MultiPhys: A Finite Element Program for Nonlinear Analysis of Continua and Structures*. CE/VPI-ST-18/02. Virginia Tech, Blacksburg, VA, 2018.

Lepage, A., Yasso, S., and Darwin, D. *Recommended Provisions and Commentary on Development Length for High-Strength Reinforcement in Tension*. SL Report 20-02. The University of Kansas Center for Research, Lawrence, KS, 2020.

Lundgren, K. Pull-Out Tests of Steel-Encased Specimens Subjected to Reverse Cyclic Loading. *Materials and Structures*, Vol. 33, August 2000, pp. 450–456.

Marques, J.L.G., and Jirsa, J.O. A Study of Hooked Bar Anchorages in Beam-Column Joints. *ACI Journal Proceedings*, Vol. 72, No. 5, May 1975, pp. 198–209.

McLean, D.I., and Smith, C.L. *Noncontact Lap Splices in Bridge Column-Shaft Connections*. WA-RD 417.1. Washington State Department of Transportation, Olympia, WA, 1997.

Moharrami, M., and Koutromanos, I. Triaxial Constitutive Model for Concrete Under Cyclic Loading. *Journal of Structural Engineering*, Vol. 142, No. 7, July 2016.

Murcia-Delso, J., and Shing, P.B. Bond-Slip Model for Detailed Finite-Element Analysis of Reinforced Concrete Structures. *Journal of Structural Engineering*, Vol. 141, No. 4, April 2015.

Murcia-Delso, J., Stavridis, A., and Shing, P.B. Bond Strength and Cyclic Bond Deterioration of Large-Diameter Bars. *ACI Structural Journal*, Vol. 110, No. 4, July 2013, pp. 659–670.

Orangun, C.O., Jirsa, J.O., and Breen, J.E. *The Strength of Anchor Bars: A Reevaluation of Test Data on Development Length and Splices*. Research Report 154-3F. Texas Highway Department, Austin, TX, 1975.

Ryu, H., Kim, Y., and Chang, S. Experimental Study on Static and Fatigue Strength of Loop Joints. *Engineering Structures*, Vol. 29, No. 2, February 2007, pp. 145–162.

Sagan, V.E., Gergely, P., and White, R.N. Behavior and Design of Noncontact Lap Splices Subjected to Repeated Inelastic Tensile Loading. *ACI Structural Journal*, Vol. 88, No. 4, July 1991, pp. 420–431.

Schrank, D., Albert, L., Jha, K, and Eisele, B. *2023 Urban Mobility Report*. Texas A&M Transportation Institute, College Station, TX, 2024.

Sheng, H., Nielson, B.G., Pang, W., and Schiff, S.D. *Precast Alternative for Flat Slab Bridges*. FHWA-SC-13-04. Clemson University, Clemson, SC, 2013.

Sperry, J., Darwin, D., O'Reilly, M., Lequesne, R.D., Yasso, S., Matamoros, A., Feldman, L.R., and Lepage, A. Conventional and High-Strength Hooked Bars—Part 2: Data Analysis. *ACI Structural Journal*, Vol. 114, No. 1, January 2017, pp. 267–276.

Tepfers, R.A. *Theory of Bond Applied to Overlapping Tensile Reinforcement Splices for Deformed Bars*. Publication 73:2. Division of Concrete Structures, Chalmers University of Technology, Goteborg, Sweden, 1973.

Virginia Department of Transportation. *Manual of the Structure and Bridge Division*. Richmond, VA, 2022.

Walker, W.T. Laboratory Tests of Spaced and Tied Reinforcing Bars. *ACI Journal Proceedings*, Vol. 47, No. 1, January 1951, pp. 365–372.

Yasso, S., Darwin, D., and O'Reilly, M. Effects of Concrete Tail Cover and Tail Kickout on Anchorage Strength of 90-Degree Hooks. *ACI Structural Journal*, Vol. 118, No. 6, November 2021, pp. 227–236.

Zuo, J., and Darwin, D. *Bond Strength of High Relative Rib Area Reinforcing Bars*. SM Report No. 46. The University of Kansas Center for Research, Lawrence, KS, 1998.